TALLINN UNIVERSITY OF TECHNOLOGY
School of Information Technologies

Fariha Afrin 184608 IVEM

INVESTIGATION OF THE FLUOROMETRY BLOCK IMPROVEMENTS POSSIBILITIES OF A FLOW CYTOMETER

Master's thesis

Supervisor: Ants Koel

Associate Professor

Tallinn 2020

TALLINNA TEHNIKAÜLIKOOL
Infotehnoloogia teaduskond

Fariha Afrin 184608 IVEM

LÄBIVOOLU TSÜTOMEETRI FLUORIMEETRIA PLOKI PARENDAMISE VÕIMALUSTE UURIMINE

Magistritöö

Juhendaja: Ants Koel

Dotsent

Tallinn 2020

Author's declaration of originality

I hereby certify that I am the sole author of this thesis. All the used materials, references to the literature and the work of others have been referred to. This thesis has not been presented for examination anywhere else.

Author: Fariha Afrin

01.05.2020

Abstract

Flow cytometry is a sophisticated technology and a powerful tool, which can measure several characteristics of a single cell, such as the size, shape, and granularity. Most of the existing Flow Cytometers (FCs) are typically large, expensive, and need experienced personnel to operate. Moreover, LAB-grade FCs rely on lasers for excitation and PMTs (or avalanche photodiodes) for detection in most of the cases. Therefore, several issues need to be solved to develop FCs that are feasible for easy integration to small LABs environments, being affordable, compact, and networked.

This MSc thesis will tackle the basic concepts of an optimal solution for the excitation sources and sensors needed for affordable & fast sensing of fluidics with acceptable precision using the fundamentals provided by previous research. The review describes several advances in excitation and detection sensors for flow cytometry over the latest years. It emphasizes focusing techniques and detection methods, which will give overall insight about excitation and detection technology for both existing and new users. The work is a contribution to the final expected outcome within PRG620 *CogniFlow-Cyte: Cognitronic Lab-on-a-Chip System for Highly-Automated Flow Cytometry*, to build an FC, which would be compact in size, with automated workflow, fast, inexpensive and easy to operate.

The experimental part follows the abovementioned project WP2 workplan – assessment of existing equipment of the Department with perspective use for high-speed fluorometry prototyping.

The thesis is written in English and 53 pages long, including 5 chapters, 27 figures, and 9 tables.

Annotatsioon

LÄBIVOOLU TSÜTOMEeTRI FLUORiMEeTRIA PLOKI PAReNDAMISE VÕIMALUSTE UURIMINE

Läbivoolu tsütomeetria on keerukas tehnoloogia ning võimas tööriist, millega saab mõõta tilga sisu mitmeid tunnuseid, nagu suurus, kuju ja detailsus. Enamik olemasolevaid voolutsütomeetreid (FC) on tavaliselt suured, kallid ja vajavad töötamiseks kogenud personali. Lisaks kasutavad laboriklassi FC-d enamikul juhtudel ergastamiseks lasereid ja tulemuse registreerimiseks PMT (fotokordisteid) või laviinfotodioode). Seetõttu tuleb modulaarsete FC-de väljatöötamiseks lahendada mitmeid küsimusi, näiteks hõlbus integreeritavus väikeste laborikeskkondadesse, sobiv hind, kompaktsus ja võrguühendused.

Käesolevas magistritöös uuritakse varasemate teadusuuringute põhjal optimaalsete lahenduste põhikontseptsioone erutusallikate ja andurite jaoks, mis on vajalikud vastuvõetava täpsusega taskukohaseks ja kiireks vedelike analüüsiks. Ülevaade kirjeldab voolutsütomeetria ergutus- ja tuvastussensorite viimaseid aastaid tehtud edusamme. Keskendutakse ergastusallika valguse suunamismeetoditele ja tuvastusmeetoditele, mis annavad üldise ülevaate nii olemasolevate kui ka uute väljatöötluste osas. Käesolev diplomitöö on panus eeldatavate lõpptulemuste saavutamisse projektis PRG620 *CogniFlow-Cyte: Kognitiivne kiiplaborsüsteem automatiseeritud voolutsütomeetria tarbeks*, et ehitada FC, mis oleks kompaktse suurusega, automatiseeritud tööprotsessiga, kiire, odav ja hõlpsasti kasutatav.

Käesoleva magistritöö eksperimentaalne osa täidab eelmainitud projekti tööpaketi WP 2 ülesannet, TJS Elektroonikainstituudi olemasoleva seadmepargi sobivuse hindamine kiire fluoromeetria prototüüpimiseks.

Lõputöö on kirjutatud inglise keeles ja pikkusega 53 lehekülge, sealhulgas 5 peatükki, 27 joonist ja 9 tabelit.

List of abbreviations and terms

AD	Analog to Digital
ADC	Analogue to Digital Converters
APD	Avalanche Photodiodes
CCD	Charge Coupled Device
CMOS	Complementary Metal–Oxide–Semiconductor
DI	Deionized
DNA	Deoxyribonucleic Acid
FC	Flow Cytometer
FCR	Flow Cytometry
FEM	Finite Element Method
FITC	Fluorescein isothiocyanate
FPGA	Field Programmable Gate Array
FSC	Forward Scattering
LD	Laser Diode
LED	Light Emitting Diode
NIR	Near Infra-Red
PD	Photodetector
PE	Phycoerythrin
PMT	Photomultiplier Tube
RNA	Ribonucleic Acid
RS	Recommended Standard
RSC	Royal Society of Chemistry
SSC	Side Scattering
TJS	Thomas Johann Seebeck
USB	Universal Serial Bus
VIS	Visible

Table of contents

List of figures

List of tables

1 Introduction

Flow cytometry is a widely used powerful technique for characterization and analysis of cells in the clinical diagnosis field throughout the world. After the Coulter cell counting discovery in 1953, optical detections were soon embraced by flow cytometry systems since the late 1960s [1]. The first developed Flow Cytometer was able to detect single parameters such as the size of the cells. In addition to that, the first instruments were often bulky and mechanically complicated. Recent instruments are relatively small and have the capability of detecting several characteristics of a cell or any other microorganisms simultaneously. The data collected from the cytometer could give valuable information about biophysical, biochemical, and molecular aspects of the cell. Fluorescence-activated flow cytometers have the capability to sort fluorescent-labelled cells from a mixed cell population. The main components of this kind of flow cytometers are fluidics, optics (excitation and sensing light paths), detection (sensorics), and presentation (microscope or data processing in computer). The fluidics is the first part that is responsible for directing liquid droplets containing investigated cells, molecules or particles, to the focused light source. Different kinds of fluorescent reagents such as fluorescently conjugated antibodies, deoxyribonucleic acid (DNA) binding dyes, viability dyes, ion indicator dyes and fluorescent expression proteins can be utilized in flow cytometry. The excitation optics focuses the light source on the cells/particles. The sensor detects the fluorescent signal from the scattered light and converts the signals to digital data that is proportional to light intensity. Finally, the computer is also needed to present and analyse the data.

The detection performance of microfluidic cytometers depends on the positioning of the particles in a precise streamline. Thus, the focused particles or cells can be detected by optical scattering-based methods, digital image processing, or non-optical methods such as impedance detection. Information is collected from forward scattering (FSC) and side scattering (SSC) in an optical detection system[2] [3]. The FSC provides information about particle size, and SSC data provide insights into the particle internal granularity. The fluorescence information can be used for immunophenotyping to distinguish among

different cell populations. Impedance-based microflow cytometers are different since the excitation is performed by using sensing electrodes within the microfluidic channel that provides insight on dielectric properties and granularity of cells [4] [5]. Digital image processing detection method is an optical imaging technique that is getting more attraction in recent research work [6] [7].

Flow cytometry can be used in various fields such as immunology, molecular biology, bacteriology, virology for organelles, nuclei, DNA, RNA, chromosomes, cytokines, hormones, and protein content investigation. Analysis of cell cycle, measurement of calcium flux, membrane potentials, and studying of the immune system are the commonly used examples of methods developed for flow cytometry. In addition, cell sorting from the cell populations is a significant application of flow cytometry.

The main challenge in flow cytometry is the development of microfabricated flow cytometers where the integration of inexpensive optical components is possible, which will be able to rapidly count cells and probe cellular populations at the single-cell level. This high throughput is necessary for the identification of different particle populations and a better understanding of the single or diverse cell population. As an example, tumour cells that are circulating in the blood can be typically present less than one per one billion cells [8]. There are some conventional flow cytometers available for the high throughput quantitation of cellular populations, they are often costly, mechanically complex, consume large sample and reagent volumes and require trained personnel for both operation and support. Hence, there is a clear need for investigation of the fluorometry excitation and detection block improvements.

1.1 Aim and Objective

The aim of this thesis is to investigate the excitation source and detection sensor for the development possibilities of Flow Cytometer. This can be achieved by objectively carrying out the following:

- Understand the concept of fluorometry for flow cytometry applications
- Study existing works that have been done and determining the level of state-of-art in the field
- Research and test plan (explained further)
- Assess the equipment available at the TJS Dept. of Electronics

- Test the performance of the overall implementation

1.2 Thesis Organization

This thesis contains introductory knowledge on Flow Cytometry (FCR), particularly excitation and detection part of an FC. The implementation and deployment information on excitation and detection blocks are then explored afterward. The first chapter of the thesis emphasizes introductory information and the intended aim of the thesis.

Chapter 2 (Background) first describes the detailed principles of FCR and fluidics. The studies covered are chosen so that possible ideas could be obtained on theoretical knowledge. The basic concept of optics and detectors are also discussed as it could be beneficial for understanding the fundamental method. The state-of-the-Art review covers the interrogation source and detector properties, the development, and the drawback of different approaches. The general discussion on design theory is also included in this chapter.

Chapter 3 (Materials and Methods) contains information on the development of the prototype of this work. Gives the description of different tools, hardware, and software used to develop the excitation and detection sensors.

Chapter 4 (Results and Discussions) The work is summed up by evaluating the results in this chapter. Several tests on the proposed sensor setup are performed. Evaluated properties include sensor sensitivity and single droplet detection at considerable speed.

Chapter 5 (Summary and Conclusions) gives a conclusive discussion of the work and future work that can be carried out.

2 Background

2.1 Principles of the Flow Cytometry

The principal components of a flow cytometer are a fluidic chamber, a light source for excitation, detector, and electronics for signal processing (Figure 1). Recent flow cytometry research has paved the way for customizable devices for particular applications.
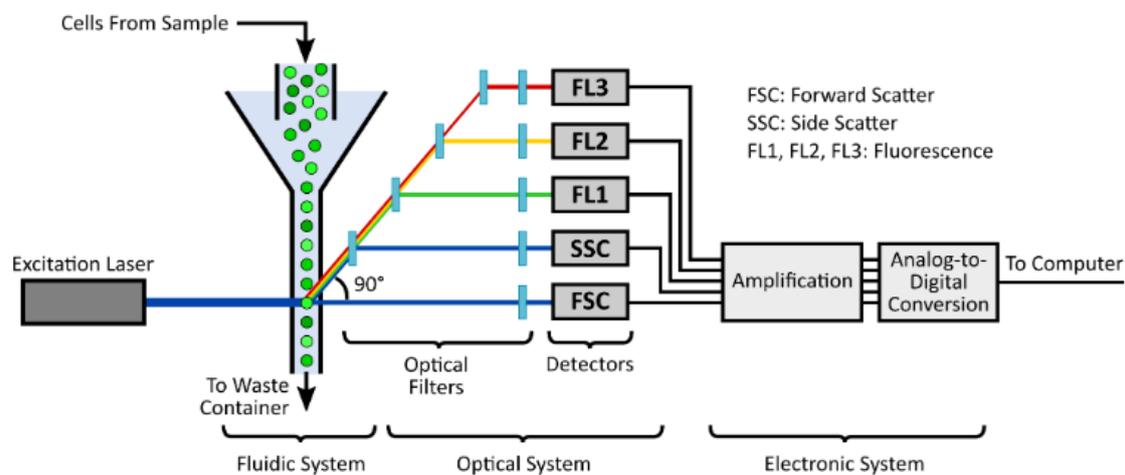
Figure 1. Schematic of a typical flow cytometer: laser beam excites the fluorescent labelled particles whose light is scattered in the forward direction (FSC) and sideways (SSC). Filters are placed before the detectors and electronics system for signal processing [9].

2.1.1 Fluidics

Fluidics is the first fundamental part of flow cytometry, which is required to measure the properties of cells or particles one by one basis. The cell interrogation process through light source requires a single particle streamline from thousands of particles, which is managed by the fluidics system. This single streamline can be achieved by using a simple pump such as a syringe pump. Initial single flow particle system was manually operated, but with the development now, the system is improved and automated. Hydrodynamic focusing system can be used for creating a single particle streamline (Figure 2). It consists of a central channel and a sheath fluid solution. The sample fluid is injected into the core channel at slightly higher pressure enclosed by outer sheath fluid, which creates a single-particle streamline.
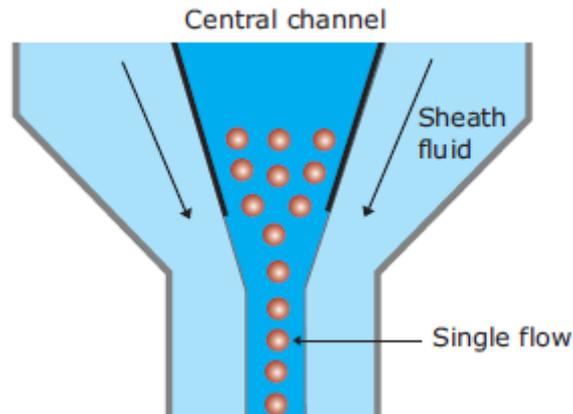
Figure 2. Hydrodynamic focusing system produces a single stream of particles where sheath fluid passes with high linear velocity than central sample flow (round particles) [10].

Obtaining single cells streamline is not possible without hydrodynamic focusing, the cuvette, or nozzle of the instrument. But this traditional hydrodynamic focusing is no longer the only option for particle focusing as researchers have explored alternative methods such as inertial focusing for microfluidic flow cytometry [11]. Microfluidics is the science or technology that processes and manipulates small (10^{-9} to 10^{-18} litres) amounts of fluids by using channels with dimensions of tens to hundreds of micrometres [12], [13]. These several methods of fluidics focusing create single-cell flow and pass through the illumination source, usually called the interrogation point, which allows single-cell analysis [14], [15].

2.1.2 Optics and Detection

Each particle from a single streamline passes through the excitation source light, which could be one or more beams of light. An optimal excitation beam is necessary to perform reliable analysis of particle because the relevant information such as size and granularity is obtained from light scattering and fluorescence emission. Detected signal intensity varies with the excitation beam intensity across the flow stream.

After the particle interrogation, light scattering is an essential parameter that could be FSC and SSC, depending on the orientation from the beam axis (Figure3). Typically, up to 20 degree offset from the light beam axis is known as the forward scatter, and 90-degree offset is side scatter which, can provide information regarding particle size and granularity or complexity respectively [10].
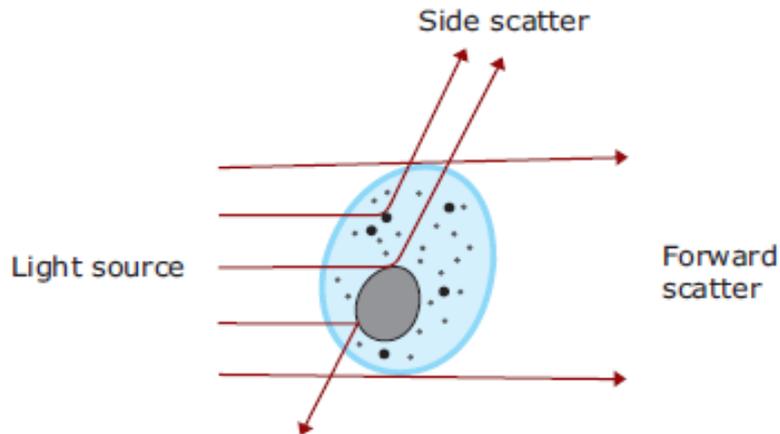
Figure 3. Diagram of cell interrogation: forward and side scatter. Particle size information is extracted from forward scattering and granularity or complexity information gathered from side scattering [10].

However, this angle depends on several factors, such as the sample characteristics, the wavelength of the excitation light, the collection angle and the refractive index of the sample, and sheath fluid. For example, if the particles are smaller than the wavelength of the illumination source, it may not scatter light in a forward direction. To get more detailed information about the particle, fluorescent labelling is generally required. Flow cytometer is capable of detecting fluorescence from properly labelled particles. Important information about the particles can be extracted from FSC, SSC, and fluorescence data.

Different kinds of laser or LED could be used as excitation light sources in flow cytometry. Lasers produce a single wavelength of light at a specific frequency which are available at different wavelengths ranging from ultraviolet to far-red and have a variable range of power levels (photon output/time typically specified in mW). The argon-ion laser is commonly used light source in FC as it can excite multiple fluorochromes. LED is another option of the excitation source, which can reduce the size and cost of the flow cytometers.

Series of optical filters, mirrors that are used to direct specific wavelengths of light and to give a shape to the light beam is a part of optics. A flow cytometer uses a combination of long pass, short pass, bandpass, and dichroic mirrors. Dichroic mirror can allow specific wavelengths to pass in the forward direction, and it can reflect the light at a 90-degree angle. Another important optics is detectors that convert the light signals into currents, which are then sent to the electronics system. The most commonly

used detector in a flow cytometer is photomultiplier (PMTs) tubes or photodiode (PD). PDs are typically used for FSC detection where the signal levels are high, and PMTs are used for side scatter and fluorescence detection because they have high gain and sensitivity. Avalanche photodiode (APD) or a Charged-coupled device (CCD) camera can also be used for the detection.

2.1.3 Signal Processing

When a particle passes through the interrogation point, light hits the particle which emits the photon. In the detector, this photon is converted to electrons, and the electronic system process this signal. The number of photons emitted is equivalent to the fluorescent light or scattered light. The principle is as the particle enters the light beam spot, the output of the detector will begin to rise, reaching to the peak output when the particle is in the centre of the light beam (Figure4).
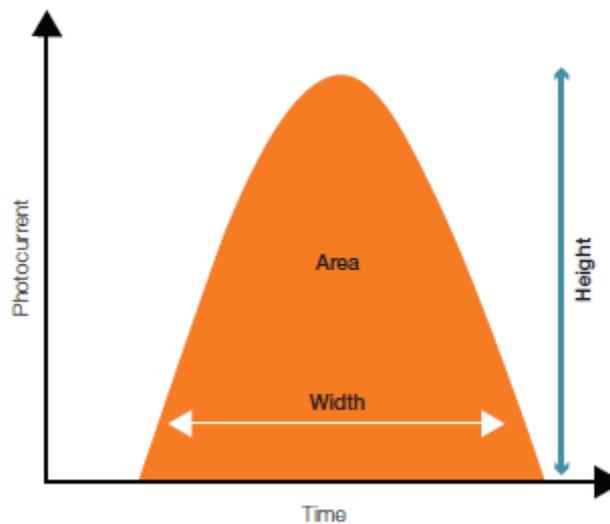
Figure 4. Pulse generated in the detector where height is the maximum amount of current output; width is the time interval during which pulse occurs, and area is the integral of the pulse. Signal intensity is measured by either height or area [16].

In this situation, the particle is fully illuminated and will produce a maximum amount of optical signal. The width interprets starting to end time of the pulse. This width could be full width above the threshold or width at half of the height level. The area is the integral of the height over width (time). The pulse magnitude of forward scattering is

roughly proportional to the size of the particle, which means small particles will create smaller magnitude and vice versa. SSC interprets particle complexity, which means decreased particle complexity will result in less light scatter and smaller pulse.

During interrogation, if there is no particle under the light beam, the output current of the detector will drop back to the baseline. However, not all signals are considered as particle information. Unwanted signals are avoided by a decision, which is made upon the predefined threshold of a dedicated detector. The determination of signal from the noise is made based upon the trigger parameter and threshold level. If the signal crosses the threshold line, it is called an "event".

2.2 Principles of Fluorescence

Apart from the forward and side scatter, particles can be separated based on light emission from fluorescent molecules. This fluorescence may appear from naturally fluorescing materials inside a particle or fluorescence-labelled antibodies. Fluorophores can be used to absorb light energy at a specific wavelength and re-emit it at a longer wavelength. The purpose of using a fluorescent marker is to directly target a particle or cell of interest and to allow its biological or biochemical properties to be measured. This phenomenon is called fluorescence, which has a wide range of applications, such as identifying the populations of cells, cell sorting and measuring enzyme activity, etc.

When light hits the fluorescence labelled particle, its electrons become excited and move from a resting state (S_0) to a higher energy state (**1**). This energy level is called an excited electronic singlet state (S_2). As there are several fluorophores available, the amount of energy required for this transition will vary fluorophore to fluorophore and its chemical environment. The typical lifetime of the excited state is 1-10 ns [16]. The electrons fall to a lower energy level, which is a more stable level called the electronic singlet state (S_1). Heat is released from this absorbed energy (**2**). The amount of heat depends on the chemical properties of the fluorochrome. Finally, the electrons fall back to their resting state (S_0), releasing the remaining energy as fluorescence (**3**) (shown in Figure 5 (A)). The difference in the wavelength of the light that excites the electrons and the light that is emitted is called the Stokes shift (Figure 5

(B)). Some fluorochromes have a small Stokes shift, and some other fluorescent compounds have large Stokes shifts.
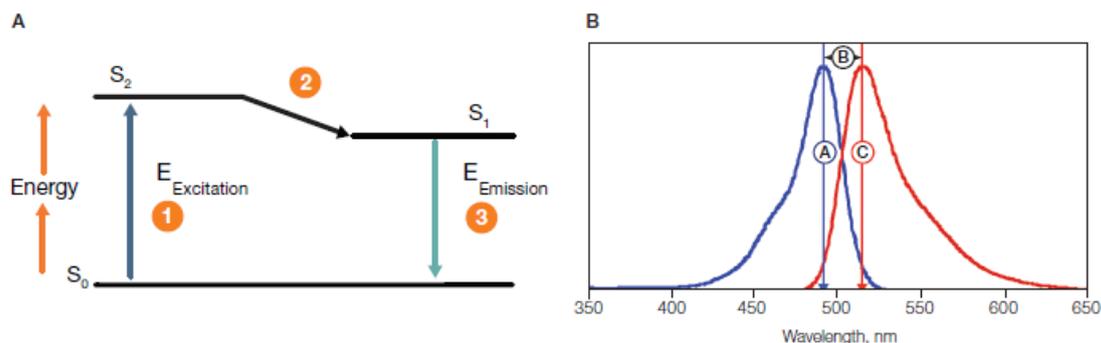
Figure 5. A, Excitation and emission stage of electrons; electrons move from the resting state, S_0, to the excited state, S_2. Some energy is released as heat, 2 and remaining energy is released as fluorescence, 3, during the movement to their ground state, S_0.B, The difference between excited emitted wavelength is called Stokes shift [16].

The wavelength of a fluorescence emission is always higher than that of excitation wavelength. There are several kinds of fluorophores available for flow cytometry, but their uses and emission spectrum depend on the type of the excitation source used. Table 1 shows some commonly used fluorophores, their excitation, and emitted wavelengths.

Table 2. Fluorochromes commonly used in flow cytometry

Fluorophore	Excitation (nm)	Emission (nm)	References
Fluorescein isothiocyanate (FITC)	488	525– 595	[17]
Cyanine dye 5 (Cy5)	633, 635	667	[18]
Peridinin chlorophyll protein/ Cyanine dye 5.5 (PerCP/Cy5.5)	488, 633, 405	655, 670	[19]
Phycoerythrin (PE)	488, 633, 405	556	[19]
Alexa Fluor	488	519	[20]

The selection of fluorochromes for flow cytometry can be made by knowing the excitation, emission properties, and binding properties of fluorescent compounds.

2.3 State of the Art

In order to research the state of the art, a search was performed in several databases, e.g., Scopus, ResearchGate, PubMed, IEEE Xplore, RSC. For a more profound understanding of the context in which this research is being carried out, it is fundamental to begin handling relevant concepts, as well as providing enough background about where the author has found opportunities to contribute with the current literature. A series of articles regarding microfluidics and FCs were found, including an overview of different sensor solutions. However, most of the articles found are regarding application-specific solutions [21] with complicated (bulky and expensive) manufacturing processes making them non-portable, expensive, and require trained personnel. An excitation laser beam excites the cells perpendicular to the flow direction and afterward both forward and side scatter intensity is measured. Most of the sensors are typically PMTs [22], [23], [24], [25]. And the optical path includes lenses, filters, and dichroic mirrors to focus and selectively filter emitted light [26]. Laser excites particles, and four fluorescence detectors made it possible to analyze the fluorescence from multiple dyes concurrently [27]. Measurement of one or more wavelengths (i.e., one or more fluorescent dyes, which each have well-defined characteristics of excitation and emission wavelengths) is possible depending on the setup. Using monochromatic, coherent light sources, and PMTs for detection enables detecting down to 50 fluorophores per particle at a flow rate of 50000 cells/s [28]. The signal processing electronics take analogue signals from the sensors and convert them by means of analogue to digital converters (ADC) with up to 32-bit resolution [22], [29]. Multiplexers, filters, and amplifiers may also be part of the circuit. The digitized signal is then processed further by an FPGA or a computer to extract and visualize spectral peaks [30]. An excitation laser with a beam scanner and a scientific complementary metal–oxide–semiconductor (sCMOS) camera has been used in imaging flow cytometry, which can detect single cells at flow rate 10,000 cells/s [31]. One or more excitation sources can be implemented in flow cytometry. A system consisting of twelve channels, three different kinds of excitation lasers, LED array for FSC, and a dedicated laser for SSC collection has been used [32]. However, the technology utilized in state-of-the-art benchtop instruments is costly (10-100 k€), large and often complicated to use [33]. Below we overview recent improvements from the literature to

system components (I) the flow cell (fluidics), (II) the sensor (excitation and detection), and (III) electronics for signal processing and novel applications (IV).

Sensor improvement (II): As referenced already, state of art FCs rely on laser beam for excitation and PMTs (or avalanche photodiodes) for detection, which is a high-speed but large and/or expensive solution [34], [35], [36]. Optical waveguides could be used to direct the light to and from the flow cell, which further limits the portability. This portability limitation is also true for typical microfluidic FCs [25]. There are some experimental microfluidic FCs rely on impedance sensors (parallel electrode layouts), but these solutions have limited spatiotemporal resolution and issues with signal-to-noise ratio [25]. The use of a spectrometer with laser excitation enables high throughput yet at the same time have limitation with cost and portability [37]. A possible novel approach is the use of LEDs as excitation sources and photodetectors (PD) or CMOS cameras as detectors [24], [38].

Using LEDs or LDs for excitation and PDs or area sensors (CMOS or CCD) for detection can make the FCs comparatively compact which, is capable of doing imaging flow cytometry (forward scattering) that not only measures cell count but also cell morphology. The optical path can be constructed from cheap parts which is another advantage but requires more sophisticated image processing than laser-PMT setups. Furthermore, due to the compactness and low price of components, multiplexing is also possible, and this way the imaging throughput of the portable system can be increased dramatically (up to ~20 kHz in theory [39]). There are outstanding issues related to sensors in portable FC which are: maximum throughput (limited also by the flow cell, presently 1-3 kHz [24]), maximum flow velocity at which individual cells are discernible (35 mm/s [39]), signal-to-noise ratio at the required sensitivity levels.

LED-camera fluorometer setups can be extremely compact, which allows device integration on smartphone platform. As demonstrated in some experimental droplet microfluidic fluorometer setups built around smartphone cameras (however, these setups are typically not high-throughput) [40], [41]. Furthermore, in LED-camera setups, 3D printed plastic frames, cheap lenses, and plastic filters are used, resulting in total costs < 1000€, which is another advantage. In addition, there are existing demonstrations of microfluidic imaging flow cytometers relying on LED-camera or LED-photodetector setups, which can detect particles of sizes ~3-5 μm [24].

Summarily, LED-camera fluorometers can provide the advantages on improvements of portability and cost. Still outstanding technical challenges must be addressed (throughput, flow velocity and signal to noise ratio), and literature examples of droplet MF FCs with LED-camera fluorometers do not exist yet.

2.4 Design Theory

In this thesis, the simplicity of designs is sought for the chance to save time and resources. The first objective is to find out the general sensitivity of the spectrometers, and one of the requirements for the setup was a stable light source. There are several light sources available that can be chosen. In this research, all the device modules available in the TJS Dept. of Electronics are used for investigation. By varying the integration time, the highest intensity is achieved for different spectrometers to understand the sensitivity. At this point, the integration time is kept in a limit where the detector won't saturate. Each measurement cycle consists of an integration part and output part. The detailed measurement method is discussed in the next chapter. The second objective is to find out the detectable speed of single droplet. A stable blue LED is used as a light source and instead of considering microfluidic chip (in existing setup, explained in the next chapter), a cuvette has been used to analyse single droplet detection speed. The reagent FITC is used for fluorescence measurement. A solution of 1:10 is prepared by diluting FITC fluorophore with de-ionized water. Since the preparation of the droplet has not been reached yet in our task plan, a sinusoidal waveform is considered (further explained later) for analysing detection speed. Each cycle of a sinusoidal signal is considered as a single droplet. This signal frequency and integration time are synchronized to find out the speed of single droplet detection and the highest number of droplets that can be detected at considerable speed. The details of the test and measurements setup are explained in the next chapter.

3 Materials and Methods

In this section, the task plan for evaluation of novel technological option for the optical path: excitation sources and detectors will be discussed in detail, starting from the requirements and explaining all the significant tasks that have been done.

3.1 Evaluation Concept

There are various approaches that could be taken to evaluate the optical path: excitation sources (number of LEDs, type, termination, yield, required material), wavelengths, replaceability, etc.), lenses (number, type, location, material), filters (number, location, material, targeted wavelength), detector (signal-to-noise ratio and sensitivity), etc. For understanding the concept, experiments have been started from the existing setup (Figure6) available in the Thomas Johann Seebeck Department of Electronics Lab-on-a-Chip workgroup. It consists of a pumping system, excitation of fluidics, and data collection.
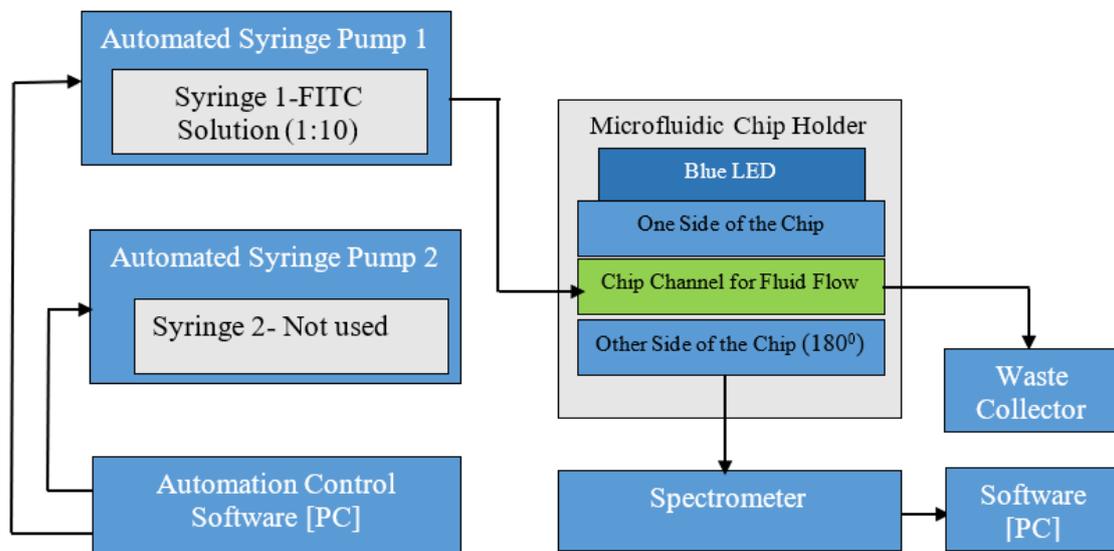
Figure 6. System diagram of existing experimental setup.

As is shown in the system diagram depicted on the above block diagram, the automation of the flow control of the syringe 1 is done using a separate syringe pump. The available syringe pump, netPumps by SpinSplit LLC, was used for the experiment. It offers a NI LabVIEW GUI, SpinStudio Flow Software, to gain simultaneous control over multiple devices using an Ethernet connection. The flow rate was 5ul/s, and experiments were

done using one reagent FITC (1:10) solution and using de-ionized water (DI-H2O). Before each experiment, the syringe, chip, and other components washed properly using DI-H2O. The forward scatter (FSC) signal was collected in the direction of the light source by using an Ocean Optics spectrometer. A LED was used in the experiment as a light source, which was blue colored (480nm). According to the fluorescence principles, the spectrum at the output should be around 540nm while using FITC solution. Using no fluorophore should show only the excitation peak, which is at 480nm. The experiment parameters are shown in Table 3.

Table 4. Description of the experiment parameter

Experiment No.	Reagent	Flow Rate [ul/s]	Integration Time [ms]	Spectrometer
1	FITC (1:10)	5	1800	Ocean Optics
2	DI-H2O	5	1800	Ocean Optics

The graph showing intensity spectra for FITC solution and DI-H2O can be seen in Figure7. The results include excitation and emission spectra collected from the spectrometer. But unfortunately, both (red and blue) spectra show small peaks during each measurement, which is not expected. To ensure that there is no false-positive fluorescence radiation coming from the used materials, experiments were repeated after cleaning and which finally lead to development of a new setup.
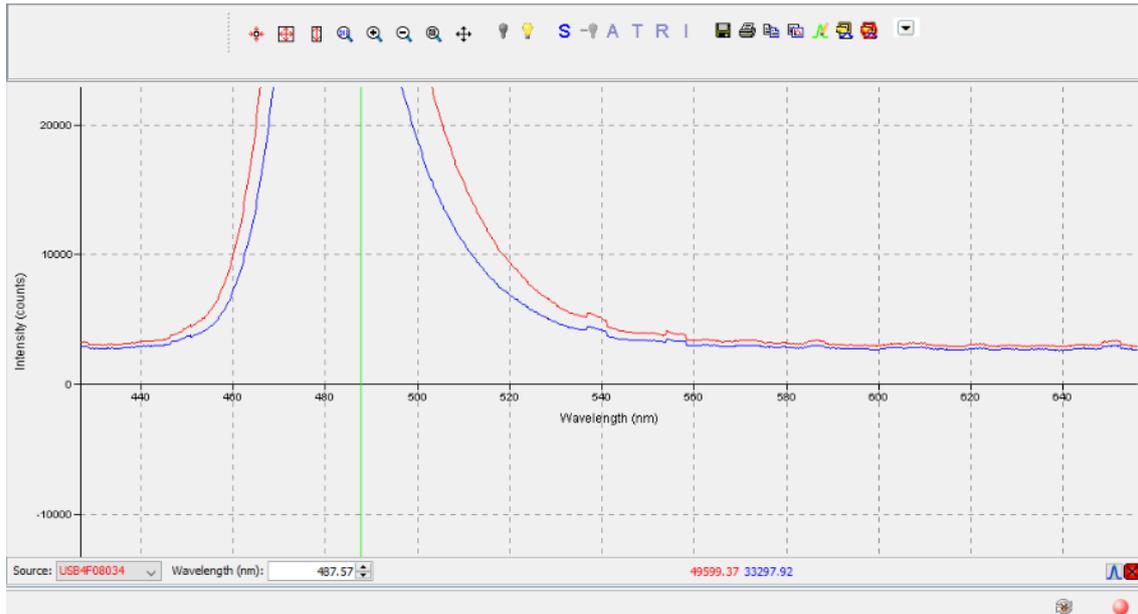
Figure 7. Wavelength vs. intensity graph showing results of the initial test: prominent excitation peak around 480nm and two small peaks around 535nm and 555nm; Blue spectra is for FITC solution and Red spectra for DI-H2O.

3.2 Evaluation Methodology for Optical Path Development

A new setup has been constructed to avoid false fluorescence radiance and to analyse the sensitivity of the spectrometers. Later, to understand the droplet detection speed capability of the spectrometers, another setup has been constructed. To reduce the time taking in measurements, the fluid flow is not considered anymore. Details of the experiment and measurement will be discussed here.

3.2.1 Sensitivity Analysis

Requirements: The required devices for sensitivity analysis have been chosen as these are available in TJS dept. of Electronics. The description of the light sources, cables, and spectrometers can be seen in Table 5.

Table 6. Description of the instruments

Requirement	Description
Spectrometer (I)	Ocean Optics spectrometer USB 4000 (Serial no: USB4E01875)
Spectrometer (II)	Ocean Optics Spectrometer USB 4000 (Serial: USB4F08034)
Spectrometer (III)	AvaSpec-2048 Spectrometer (Serial no: 0802058U1)

Spectrometer (IV)	Hamamatsu H-micro series spectrometer C12880MA (Electrical board (C13016-01), Sensor board (C13016-02))
Light Source (I)	Avantes Hal-Cal mini (MINAKO VV28129; S/N:LS-1901003)
Light Source (II)	Avantes Hal-Cal (MINAKO-PV005535 K151525; S/N: LS-0712024)
Fiber Optic Cable (I)	Ocean Optics cable P400-2-VIS-NIR (Serial: EOS-438293-52)
Fiber Optic Cable (II)	Ocean Optics cable (Serial: EOS-42101-25)
Fiber Optic Cable (III)	Avantes FC-200UC (Serial: 0801085)

The operating principle of the spectrometer is that the light enters through an entrance slit and is diversified. Then this divergent light is collimated by a curved mirror and scattered into spectral components by the diffraction grating. Each of these wavelengths is reflected at a different angle and imaged onto discrete pixels of a detector using another concave mirror. A spectrum is obtained from the detector, which is a charge-coupled device sensor (CCD image sensor) output. Figure 8 shows the light path of Ocean optics and Avantes spectrometer.
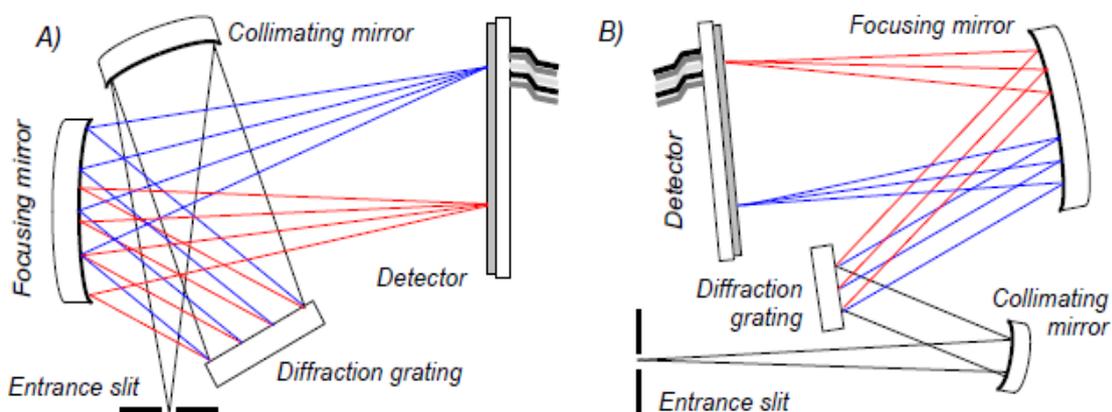
Figure 8. Image of the operating principles of the spectrometer (A: Ocean Optics Spectrometer, the light paths are crossed over the optical components) and (B; Avaspec spectrometer, the light paths are not crossed) [42].

The main difference between Hamamatsu spectrometer and previously mentioned two spectrometers is the sensor type. Hamamatsu uses CMOS linear image sensor (Figure9) for detection. After the entrance of light through the slit, it reflects from the diffraction grating and is directed to the CMOS linear image sensor, which then converts the diffracted light into voltage.
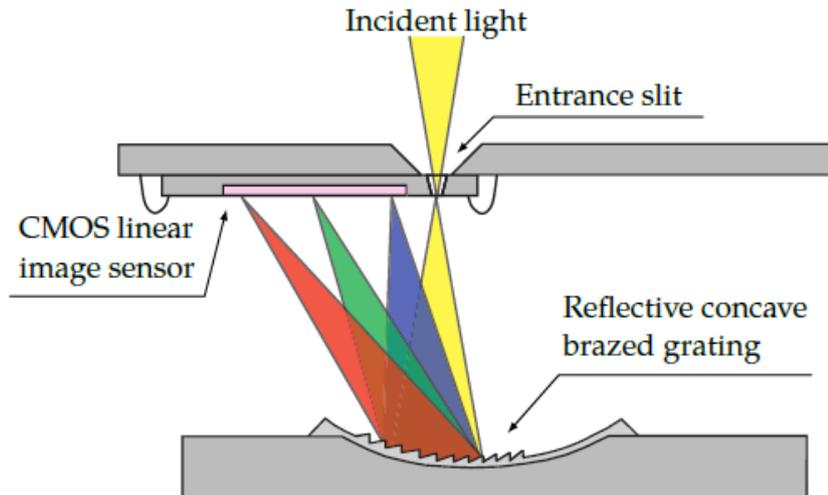
Figure 9. Image of the light path and optical components layout of the Hamamatsu spectrometer [43].

The specifications of the spectrometers and light sources (Table 7) were laid out from manufacturer datasheets, taking into account the experimental requirements and also the common good practice. It is useful to know the spectral range and other information of the spectrometers and light sources for further experiments as well.

Table 8. Specification summary of the spectrometers and light sources [44], [45], [46], [47], [48]

Spectrometer and Light Source	Specification					
	Dimension [mm]	Detector	Detection Range [nm]	Power supply [W]	Integration time	Interfaces
Spectrometer (I) & (II)	89.1 x 63.3 x 34.4	3648-element linear silicon CCD array	200-1100	1.25	3.8 ms to 10 seconds	USB 2.0, RS-232
Spectrometer (III)	175 x 110 x 44	CCD linear array	200-1100	5.28	2 msec – 60 seconds	USB 1.1, USB 2.0, RS-232,
Spectrometer (IV)	Control Board:90 x70 Sensor	High sensitivity CMOS linear image sensor	340-850	0.03	11-1000000us	USB 2.0

	Board:30 x44					
Light Source (I)	150 x 78 x 37	-	350-1095	24.96	-	-
Light Source (II)	132 x 110 x 44	-	350-1095	28.80	-	-

Method: Using a stable light source is required to get precise data from the spectrometer. Two available stable light sources (Avantes Hal-Cal and Avantes Hal-Cal mini light source) have been used to evaluate the sensitivity. The basic block is shown in (Figure 10).
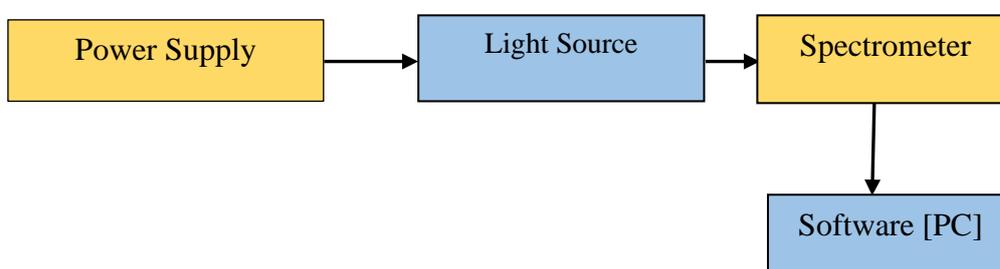
Figure 10. Generic schematics of the spectrometer's sensitivity configuration.

Description: The basic operating principle of this setup is that the light passes through the optical fiber, which enters into the spectrometer through an entrance slit, and the spectrum is obtained from the detector output. The equivalent input light intensity is measured at different integration times. Integration time is the length of the time at which detector in the spectrometer can capture light. Longer integration time results raise the intensity of the signal. This integration time range varies from spectrometer to spectrometer. Finally, data collection and powering of the spectrometers is achieved via USB connection to laptop computers (USB2.0 for all measurements). The measurements have been recorded for each combination from four spectrometers, two light sources, and three optical cables. These analyses also include finding powerful light source and the optical cable with highest transmission in visible light range..

Figure 11shows the device connection setup for spectrometer sensitivity analysis where the Hamamatsu spectrometer (showed in red arrow) is connected with Avantes (HAL CAL Mini) light source (showed in blue arrow) through an optical fibre. A USB from the spectrometer is connected with the laptop for spectral measurements.
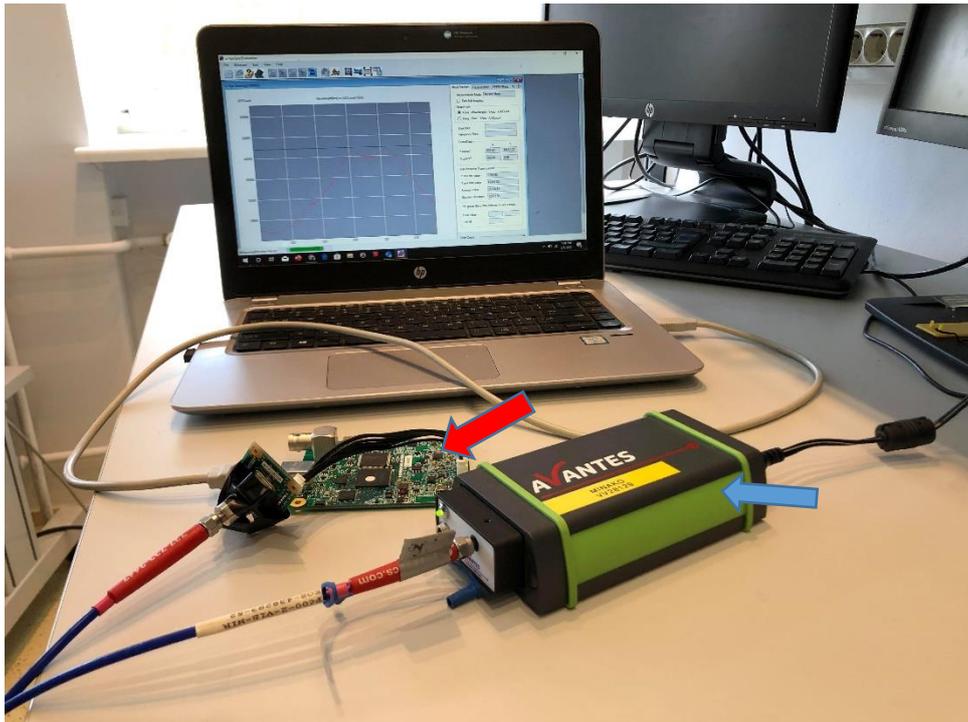
Figure 11. Image of the setup of sensitivity analysis.

The same setup has been repeated for different spectrometers and light sources.

3.2.2 Droplet Detection Speed Analysis

In droplet-based microfluidic flow cytometry, droplet detection speed is an important aspect. For droplet detection speed analysis, a setup has been constructed.

Requirements: The fundamental instrument requirements for the setup are shown below in Table 9.

Table 10. Summary of Requirements

Requirements	Quantity	Description
Excitation Source	1	LED 480nm
Spectrometer	4	Spectrometer (I), (II), (III) and (IV)
Sample	-	FITC and DI water solution (1:10)
Cuvette	1	Dimension: 45mmx12.5mm Size
Filter	1	FGL530nm filter
Cable	2	Fiber optic cable and USB

Oscilloscope	1	Agilent DSO-X 2012A Digital Storage Oscilloscope
Power Supply	1	Keysight E3630A Triple output DC Power Supply
Signal Generator	1	Agilent 33120A Function / Arbitrary Waveform Generator

Method: The strategy is to analyze the capability of the spectrometer in high throughput droplet detection. Instead of using droplets, an equivalent sinus wave has been considered to minimize the time and cost during the analysis (Figure12).

(a) Droplets

(b) An equivalent sinusoidal signal
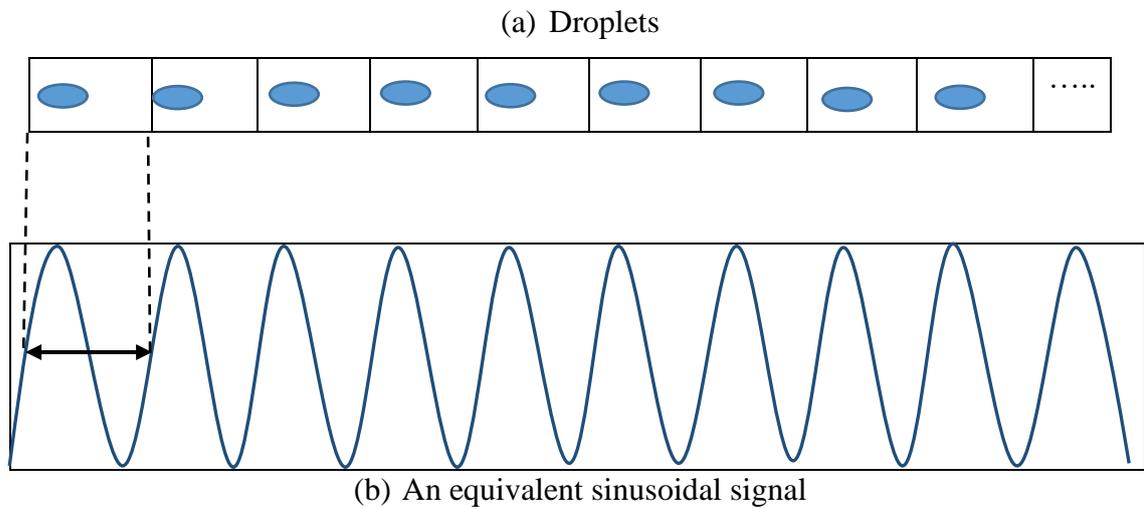
Figure 12. The principle strategy for visualizing the droplets (a) Representation of single droplets (b) A sinusoidal wave represents the state of each droplet in one cycle.

Description: The analysis was performed using the following system setup (Figure13), which includes signal generation, interrogation of point, and placement of the spectrometers.
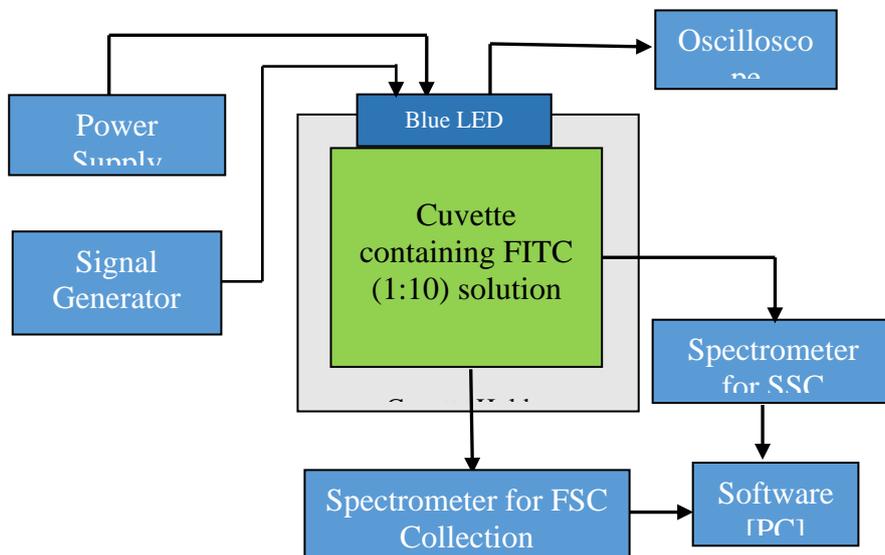
Figure 13. Generic schematics of droplet detection speed configuration.

The setup consists of three main parts: an illumination part, microfluidic, and spectra collection part. In the illumination part, a blue LED is attached with a cuvette holder using glue to act as a focused light source. The cuvette (Figure 14) containing FITC (1:10) solution is fully covered with the lid to stop any evaporation.
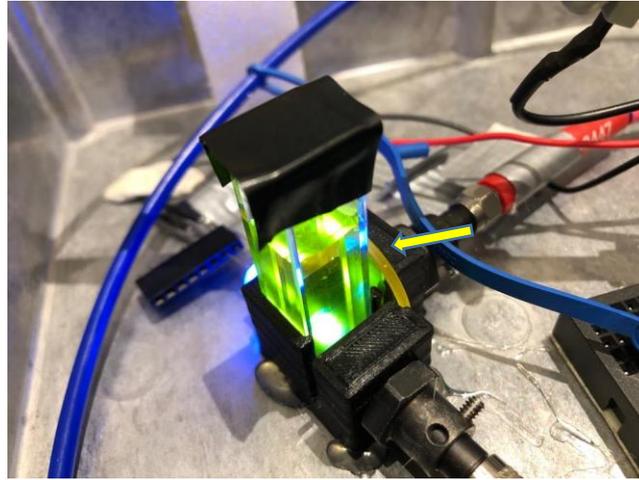
Figure 14. Image of the cuvette made of high-performance quartz glass containing FITC (1:10) solution, a 530nm glass filter (location marked with yellow arrow) is attached in 90^0 angles of the light source.

There were two available channels for collecting the scattered signal by the spectrometer. The forward scatter (FSC) signal was collected in the direction of the light source and side scatter (SSC) at a 90^0 angle to the excitation light source by using fiber optic cable. But SSC spectra were considered for experimental analysis as it suppresses the excitation signal much. The prototype constructed for the evaluation was kept in an enclosure box to keep isolated from outside light.
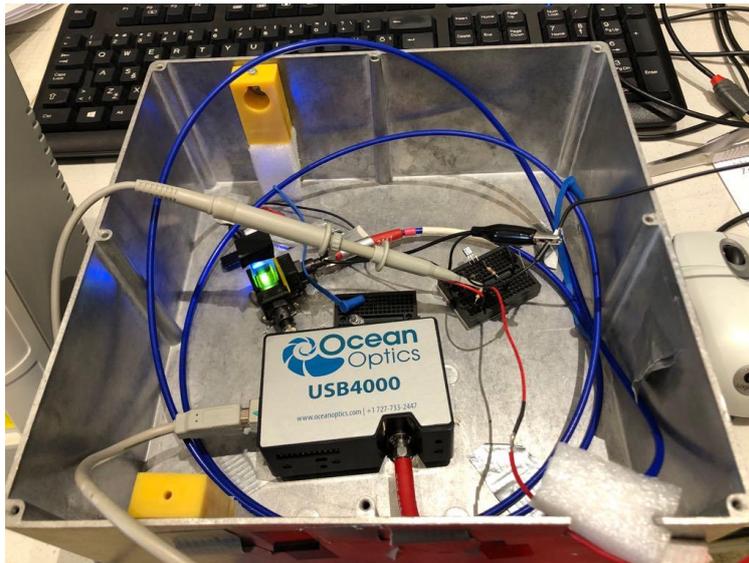
Figure 15. Image of the prototype enclosure consisting of Ocean optics USB4000 spectrometer, LED driver circuit, cuvette surrounding filter and light.

This LED is controlled by a signal generator (Agilent 33120A Function / Arbitrary Waveform Generator) and power supply (Keysight E3630A Triple Output DC Power Supply).
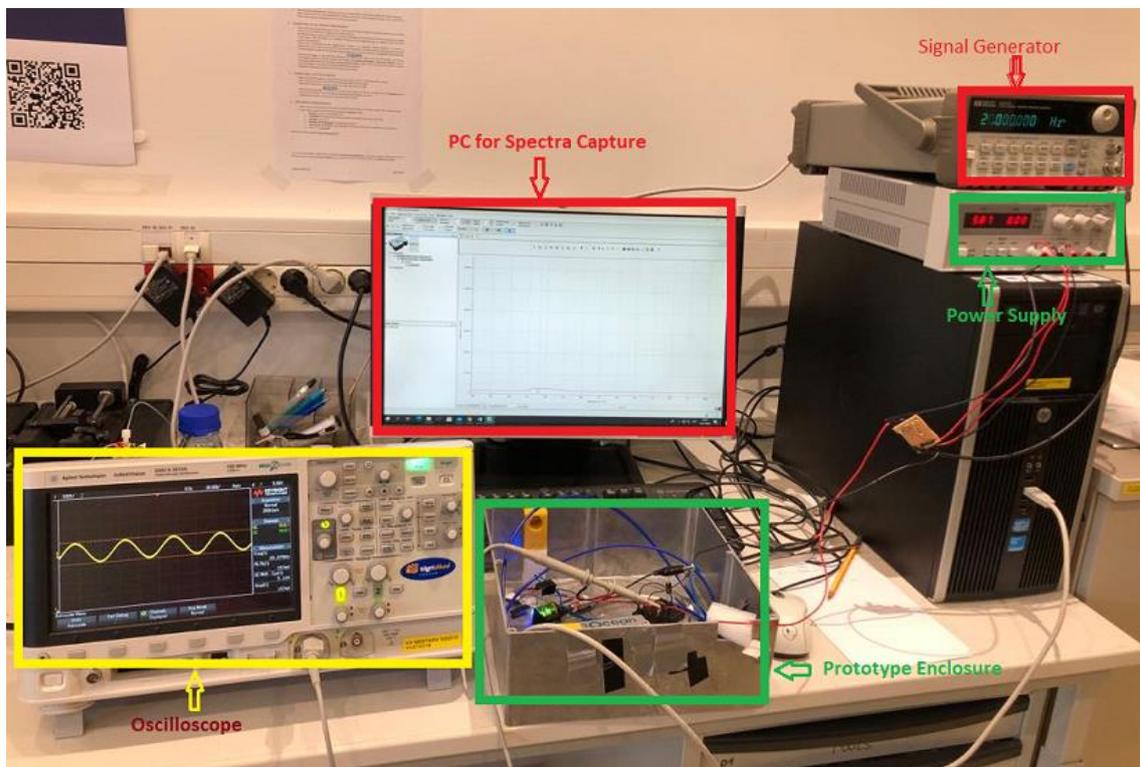
Figure 16. Experimental setup showing signal generator and power supply at the right side, an oscilloscope, a PC and prototype enclosure consisting of LED, cuvette and spectrometer.

Toward the start, LED current level (maximum and minimum current) is determined by using the voltage source. This minimum and maximum current level is required for signal offset from the signal generator. Maximum current is 19.9mA which is determined at voltage 5.50V. To find out the minimum current, voltage is reduced from 5.50V. The minimum current is determined which is 0.03V at 2.89V. There are some internal voltage drops, henceforth an oscilloscope (Agilent DSO-X 2012A Digital Storage Oscilloscope) is also used to measure the maximum and minimum voltages during this time (Maximum voltage: 4.75V and minimum voltage 2.35V). The center voltage is calculated from this minimum and maximum voltage which is 1.2V. The supply voltage is set to this center voltage level. Lastly, these two voltages (maximum and minimum voltage) are used to keep the sinusoidal wave in this range. A sinusoidal signal is generated from the signal generator, which has peak to peak voltage 2.4V. Keeping the amplitude constant, the frequency has been changed for synchronization with spectrometer integration time. The light from the LED interacts with solution in cuvette. Then the illuminated light passes through a 530nm glass filter (showing with a yellow arrow in Figure 17), which is captured by spectrometer's detector. A computer is used to read out the spectral data from the spectrometer. For the analysis purpose, the maximum, minimum frequency has been found out and recorded.

3.2.3 Electronics Design

Using LED as a light source requires constant current supply to obtain stable luminous intensity for particle interrogation. It also provides an advantage to place multiple LEDs in series. This is because the current-controlled system lowers or raises the voltage to control the current. Moreover, a great variety of regulators can be applied this way, and that only one terminal connects the regulator to the LEDs.

The schematic (Figure 18) shows the use of a regulator (LM317) and resistors to control the LED current. The purpose of using the Arduino nano board is to control the blinking interval according to the requirement. A 12V battery has been used for power supply. Resistor value determination is quite simple. The output voltage of the LM317 regulator is 1.25V, and the maximum drive current of LED is 1A, which is mentioned in the datasheet.

$$\text{So, } R = \frac{V}{I} = \frac{1.25\,V}{1\,A} = 1.25\,\Omega$$

Where *V* is the output voltage of the regulator,

I is the current drive in LED and

R is the required resistor value
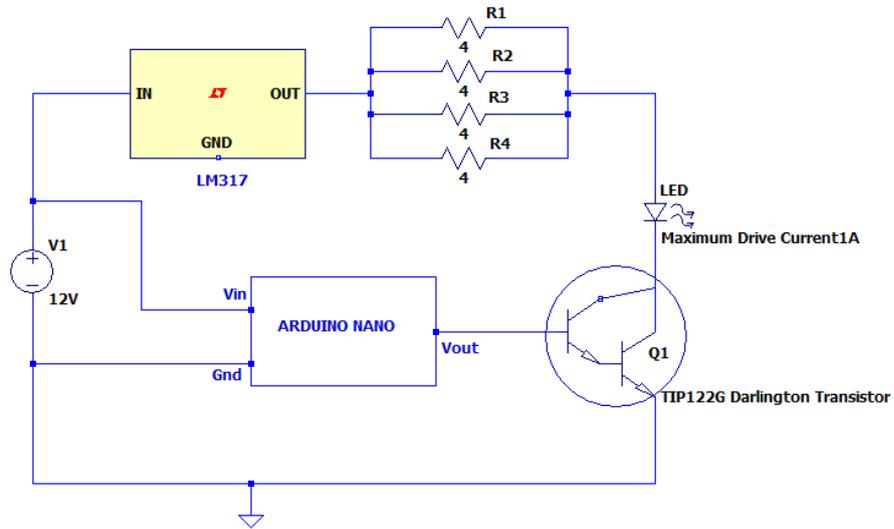
Figure 17. Schematic of the LED driver circuit with constant current regulator.

For assembly, the regulator, resistor, and Darlington transistor are welded to a radiator board. Instead of using one single resistor, four parallel resistors have been used. Also, a pinboard is used to assemble the Arduino nano board, power source, radiator board, and the LED. Finally, all these are put together in an enclosure box.
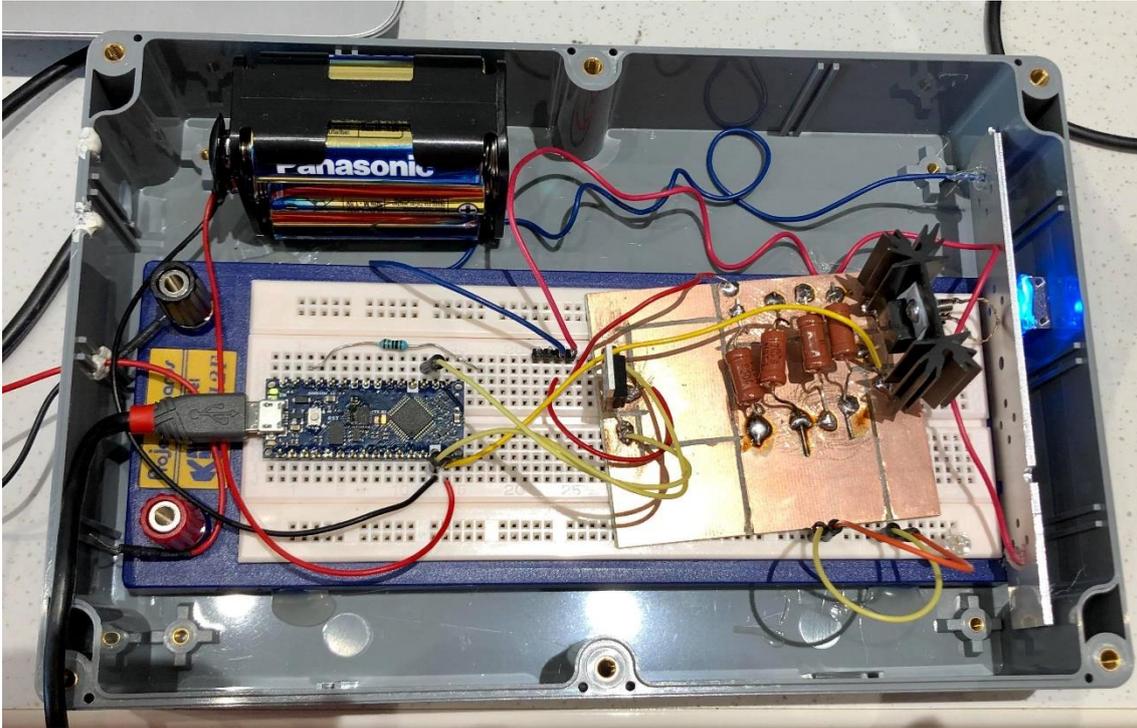
Figure 18. Image of the assembled LED driver circuit.

3.2.4 Software and Communication

A vendor-specific software package is available with all spectrometers that can be used for control and data aquisition. To ensure automated test, control, measurement, and also for multiple device integration, a common vendor neutral development environment is necessary. This allows quick data capture for simple measurement to a large system with complex architectures. Thus, it is necessary to check the availability of tentative programming development options for the spectrometers.

Table 11. Summary of programming environment of the Spectrometers

Spectrometer	Development Programming Language
Spectrometer (I) and (II)	C, C++, C#, Delphi, Java, LabVIEW, Visual Basic, Excel, MatLab
Spectrometer (III)	Borland C++ Builder 5.0, Borland Delphi 6.0, Embarcadero C++Builder 2009, Embarcadero Delphi 2009, LabVIEW 8.2, older versions on request, MATLAB 7.1 R14 SP3, Microsoft Visual C++ 2008 combined with the Qt4 framework, Microsoft Visual Basic 2008, Microsoft C# 2008, Microsoft Visual C++ 2008

Spectrometer (IV)	Microsoft Visual Basic, Matlab

As mentioned in Table 12, controlling of a spectrometer could be done using several connection methods. For the purpose of future automation, Labview and Matlab have been used beside spectrometer default software. Following Figure 19 shows the spectra collected by default software and Matlab 2019. For this measurement, Avantes Hal Cal mini light source has been used and directly connected with Ocean optics USB 4000 spectrometer.
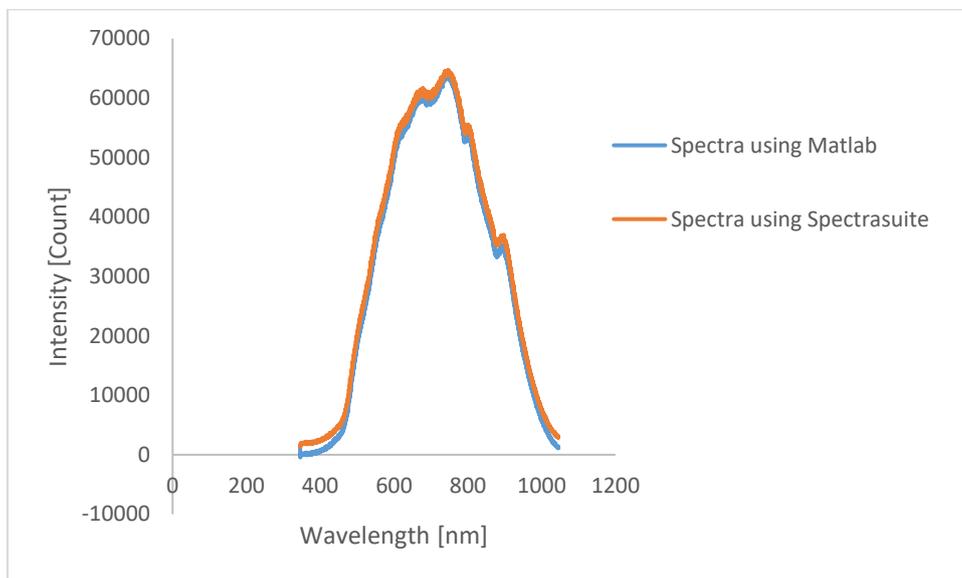
Figure 19. The recorded spectra of Ocean optics spectrometer at integration time 170ms; Red plot is taken using default software and blue plot is in Matlab.

There are no noticeable changes in the spectra, but Matlab allows to take measurements from multiple spectrometers at a time while Spectrasuite allows only one device.

4 Results and Discussions

To discuss the results of two different evaluation processes, experimental results will be presented and analysed in succession.

4.1 Results and Analysis of Sensitivity Setup

The measurement of the experiments has been recorded for all available devices. Thus, it creates 18 combinations of the devices (which can be seen in Table 13). The first idea was to take the measurements for finding maximum providable integration time where the signal is not saturated but reach to the peak. But it seems not feasible to compare the sensitivity of the spectrometers effectively. Later an intensity level has been chosen to keep the integration time constant for a specific spectrometer. The recorded data is presented in the Table.

Table 14. Intensity or ADcount measurement data for different combination of spectrometer, light source and optical fiber

Spectrometer	Optical Fiber	Light source	Integration Time [ms]	Intensity or ADcount
Ocean optics spectrometer (I)	(I)	(I)	100	32042.52
	(I)	(II)	100	42485.11
	(II)	(I)	100	30139.96
	(II)	(II)	100	41383.30
	(III)	(I)	100	18783.97
	(III)	(II)	100	26291.82
Ocean optics spectrometer (II)	(I)	(I)	100	40140.19
	(I)	(II)	100	53222.61
	(II)	(I)	100	39417.25
	(II)	(II)	100	53157.08
	(III)	(I)	100	22916.77

	(III)	(II)	100	31200.80
Avantes Specrometer (III)	(I)	(I)	10	31512.15
	(I)	(II)	10	43967.92
	(II)	(I)	10	31015.77
	(II)	(II)	10	42715.62
	(III)	(I)	10	27597.38
	(III)	(II)	10	41088.23
Hamamatsu spectrometer (IV)	(I)	(I)	0.5	43514.19
	(I)	(II)	0.5	54063.08
	(II)	(I)	0.5	43118.60
	(II)	(II)	0.5	55381.32
	(III)	(I)	0.5	18460.56
	(III)	(II)	0.5	22943.84

It can be seen from the Table that Ocean optics specrtrometer is giving around 40000 ADcount for 100ms integration time where Avantes spectrometer is giving the same level of intensity for 10ms integration time. And the integration time is 0.5ms for Hamamatsu spectrometers, where the intensity is same. These intensity level varies a little bit for different combinations of devices. The spectra obtained for the best combination of devices are shown here for the result evaluation.

In Figure 20, the light intensity varies with wavelength can be seen. The spectra start rising at 400nm and peak value obtained at 665nm wavelength. This peak intensity is measured using the software scale, which is 42485.11 counts. The integration time for this measurement was 100ms.
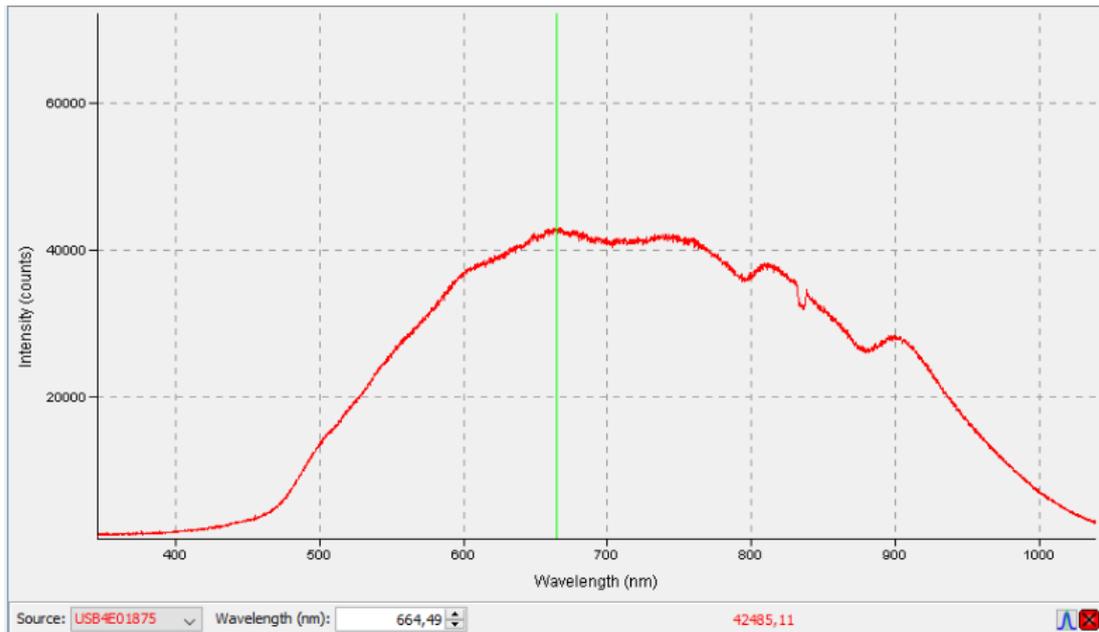
Figure 20. Intensity spectra shows peak intensity count 42485.11 at integration time 100ms; Used devices are Ocean optics spectrometer(I), Avantes light source (II) & optical fiber (I).

The integration parameter was same for this measurement as well. Slight change in peak intensity can be seen in (Figure 21) comparison with previous spectra. The peak is obtained at 667.54 nm to 770nm wavelength and slight drop is noticeable at the middle. Moreover, the intensity count is approximately 10000 count higher.
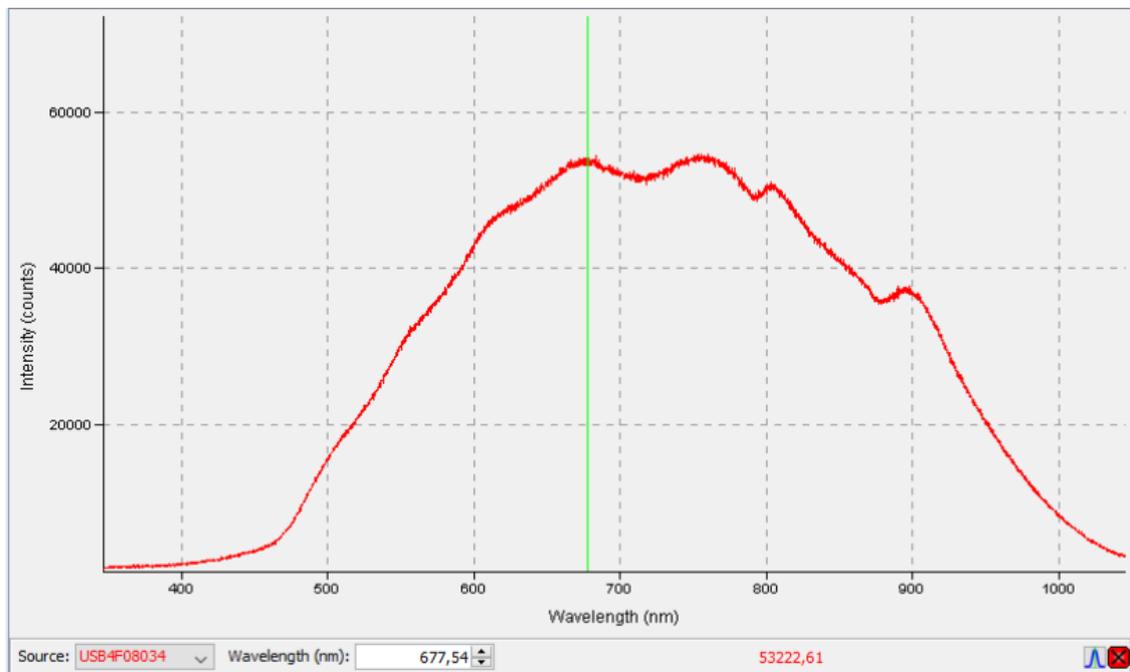
Figure 21. Intensity spectra shows peak intensity count 53222.61 at integration time 100ms; Used devices are Ocean optics spectrometer (II), Avantes light source (II), and optical fiber (I).

For Avantes spectrometer the spectrum range is similar with Ocean Optics spectrometer, but a sharp fall is noticeable in between two peaks. One peak is obtained at around 590nm and another at 700nm (Figure 22). The peak intensity count is 43967.92 for integration time 10ms.
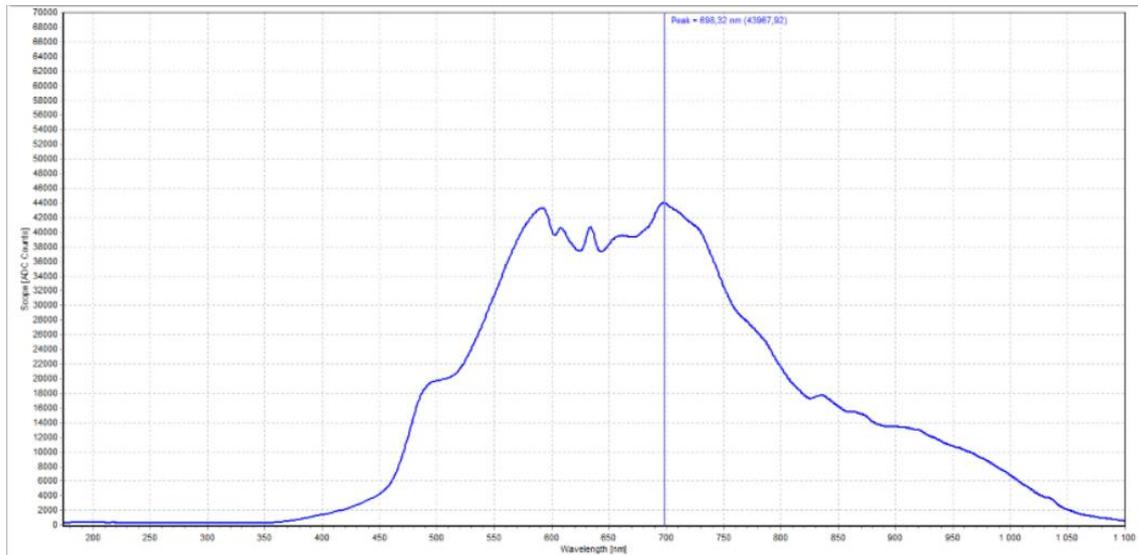
Figure 22. Intensity spectra show peak intensity count 43967.92 at integration time 10ms; Used devices are Avantes spectrometer (III), Avantes light source (II) & optical fiber (I).

To obtain the same level of intensity count, the integration time is given 0.5ms. The intensity is higher than the other three spectrometers for such low integration time. The peak starts from 630nm and stays until 770nm, which has a slight fall in the middle. The main difference with previous spectra is the spectral range. The spectra start from 340nm and end at 850nm; this is because of the spectral range of the Hamamatsu spectrometer.
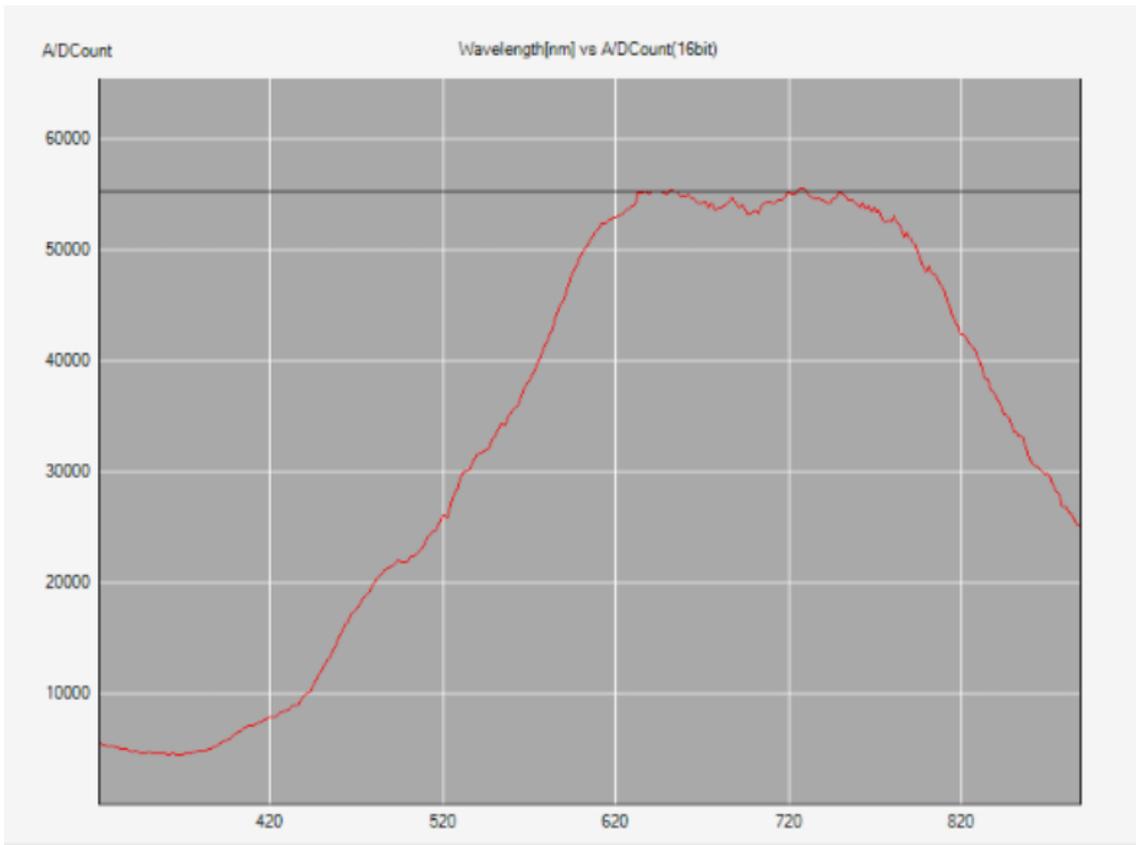
Figure 23. Intensity spectra shows peak intensity count 55381.69 at integration time 0.5ms; Used devices are Hamamatsu spectrometer (IV), Avantes light source (II) & optical fiber (II).

Table 15. Recorded intensity for best combination of devices

Spectrometer	Optical Fiber	Light source	Integration Time [ms]	Intensity or ADcount
Ocean optics spectrometer (I)	(I)	(II)	100	42485.11
Ocean optics spectrometer (II)	(I)	(II)	100	53222.61
Avantes Specrometer (III)	(I)	(II)	10	43967.92

Hamamatsu spectrometer (IV)	(II)	(II)	0.5	55381.32

The device details, parameters (integration time) and intensity count has been included (Table 16) only for the best combination. The first observation is that all the spectrums are in the highest intensity for the light source (II), which indicates it is more powerful than the light source (I). Though both light sources have the same bulb output, fiber optic cable (I) turned good for the first three spectrometers, but optical fiber (II) seemed good for Hamamatsu spectrometer. The main observation is that Avantes spectrometer is 10times more efficient than Ocean Optics spectrometer since Avantes Spectrometer provides similar intensity for 10ms integration time while Ocean Optics provides in 100ms integration time. And Hamamatsu spectrometer provides same level of intensity for 0.5ms integration time thus it is 20 times more efficient than Avantes spectrometer.

4.2 Results and Analysis of Droplet Detection Setup

As demonstrated earlier that the equivalent droplet was determined by using a sinusoidal signal generator. The frequency and integration time were manually kept the same to determine single droplet detection speed. For example, if the integration time is 25 microseconds, the frequency is considered to be 40 KHz, which indicates the detector can detect a single droplet in 25 microseconds or 40000 droplets in 1 second.

The sample we used is FITC (1:10) solution and blue excitation light (480? Nm), which interaction should produce green light (520-560nm) spectra. To cut off the unwanted excitation signal, a lowpass glass filter (530nm) was set on sensing path. The maximum and minimum diode lighting frequency has been recorded to understand the spectrometer capability in detecting the maximum number of droplets with considerable speed.

Initially, the tests have been done for minimum frequency and then for maximum frequency. The intensity is at the highest peak is achieved for minimum frequency where the spectra reaches to the peak but not saturated. 10% and 70% of the maximum intensity is calculated and corresponding spectra recorded. The graphical representation for the Hamamatsu spectrometer is shown in Figure 24. The highest intensity is

obtained at 109.89 Hz, and the lowest intensity is obtained at 5KHz frequency. The peak intensity count is 61051 and 4581, respectively. The yellow plot shows 70% of the intensity of maximum and grey interprets 10% of maximum intensity. The spectral width is 216 nm, which starts rising from approximately 490nm and ends at 706nm. The possible detection range shows in the graph is 323nm to 888nm.
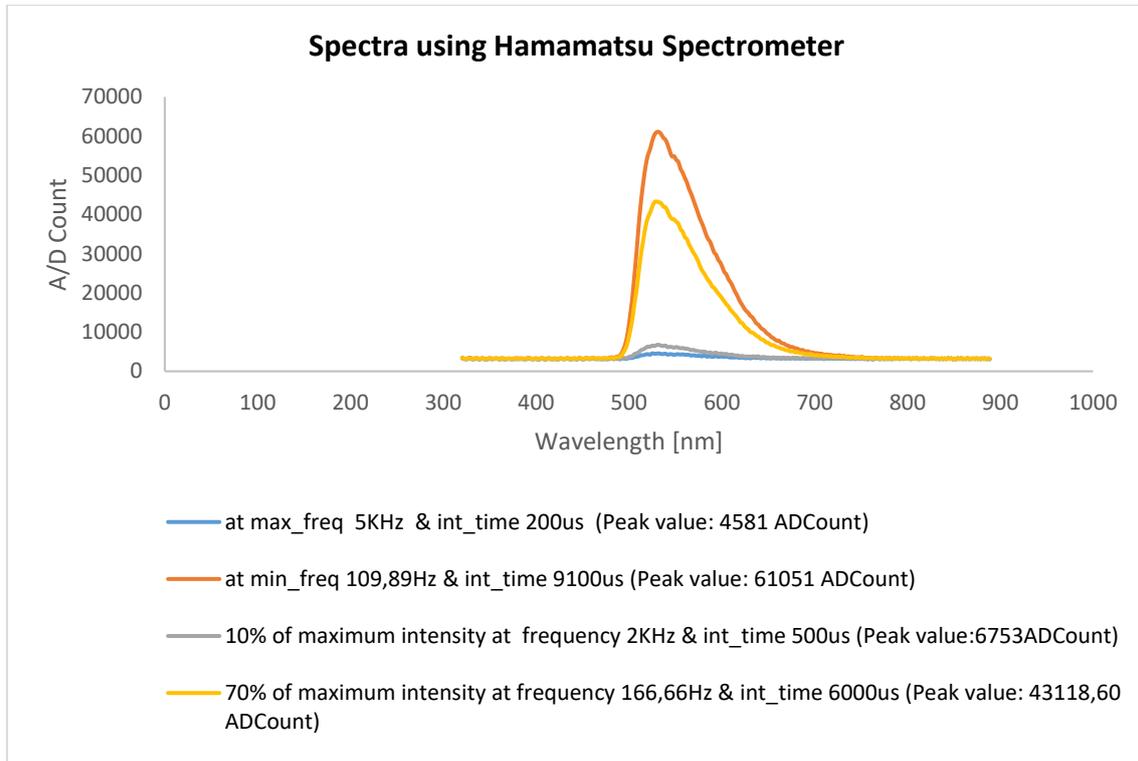
Figure 24. The spectrum captured using Hamamatsu spectrometer (IV), the highest intensity is obtained at 109.89 Hz, and the lowest intensity is obtained at 5KHz frequency. The yellow plot shows 70% of the intensity of maximum and grey interprets 10% of maximum intensity.

The spectra shown in Figure 25 is recorded by using 'Avasoft' software, which is provided with Avantes spectrometer. The highest and lowest intensity is obtained at a frequency of 6.25 Hz and 500Hz respectively. The corresponding peak intensity count is 59557.38 and 784.62, respectively. The blue plot shows 70% of the intensity of maximum and yellow interprets 10% of maximum intensity.

In comparison with previous measurement results, the lower frequency is approximately 17 times lower in this case. On the other hand, higher frequency is ten times lower than the previous measurement result, which indicates Hamamatsu spectrometer has better detection speed properties (higher sensitivity) than Avantes spectrometer. The spectral

range is similar for both measurements. In this case, spectra start rising at 490nm and end at 709nm, which results spectral width 219nm. The detection spectral range is higher than Hamamatsu spectrometer, which is 178nm to 1098nm.
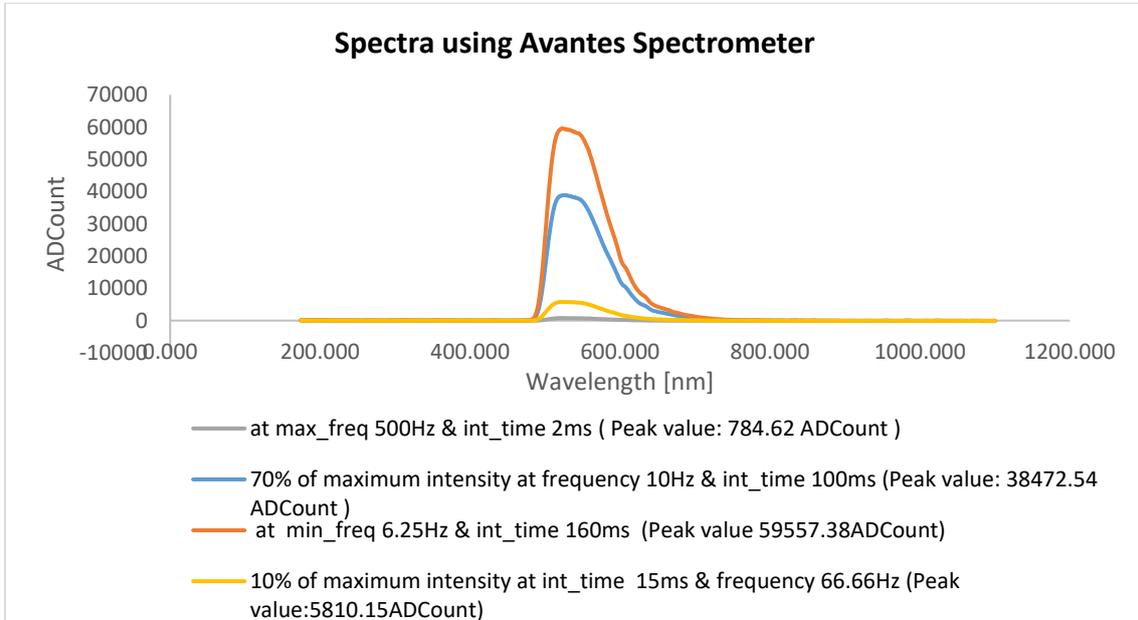

Figure 25. The spectrum captured using Avantes spectrometer (III), the highest intensity is obtained at 6.25 Hz, and the lowest intensity is obtained at 500Hz frequency. The blue plot shows 70% of the intensity of maximum and yellow interprets 10% of maximum intensity.

The spectra shown in Figure 26 is recorded by using 'SpectraSuite' software which is provided with Ocean Optics spectrometer. The highest and lowest intensity is obtained at frequency 6.6Hz and 20Hz, respectively. The corresponding peak intensity count is 7294.86 and 3061.71, respectively. The grey line shows a 70% intensity of the maximum intensity. 10% of the maximum intensity is not achievable as corresponding integration time can't detect any droplet.

In comparison with Figure 25, the lower frequency is approximately the same, but the higher frequency is 25 times lower. The spectral range is similar for both measurements. In this case, spectra start rising at 490nm and end at 712nm, which results in spectral width 222nm. The detectable spectral range is also approximately the same, which is 347nm to 1044nm.

Spectra using Ocean Optics Spectrometer_1

Legend:
- at max_freq 20Hz & int_time 50ms (Peak value:3061.71 ADCount)
- at min_freq 6.6Hz & int_time 150ms (Peak value: 7294.86ADCount)
- 70% of maximum intensity at frequency 8Hz & int_time 120ms (Peak value:5001.14ADCount)
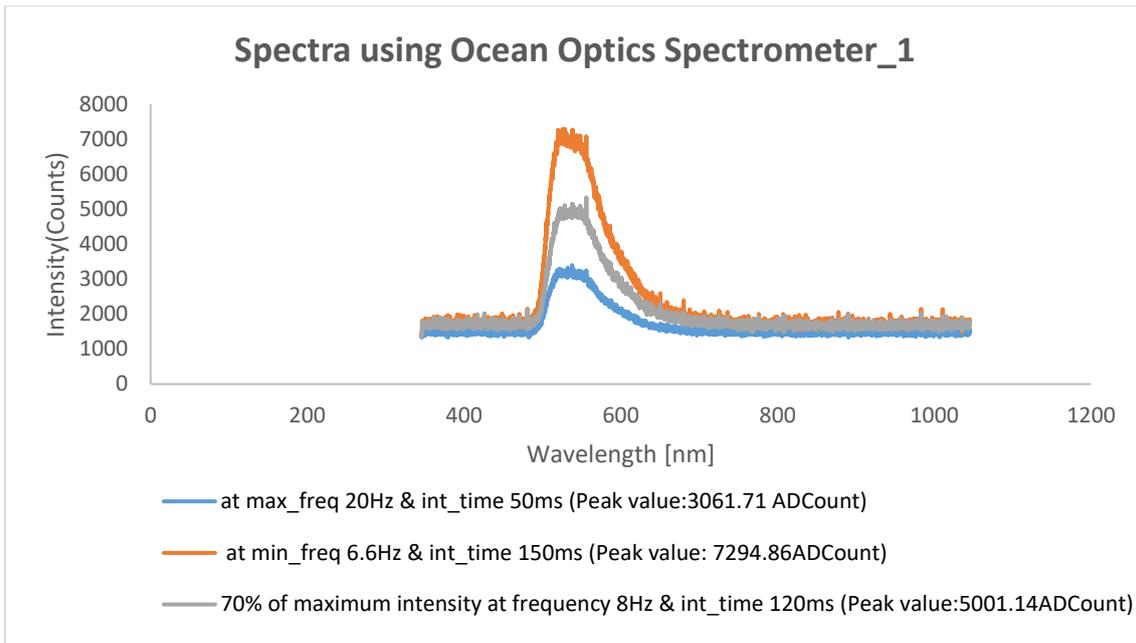
Figure 26. The spectrum captured using Ocean optics spectrometer (I), the highest intensity is obtained at 6.6 Hz, and the lowest intensity is obtained at 20Hz frequency. The grey plot shows 70% of the maximum intensity.

The spectra shown in Figure 27 is also recorded by using 'SpectraSuite' software, which is provided with Ocean Optics spectrometer. The only difference with the previous measurement is another model of Ocean Optics spectrometer is used in this case. This second Ocean Optics spectrometer provides the highest and lowest intensity at the same frequency 6.6Hz and 20Hz, respectively. The corresponding peak intensity count is 5859.24 and 2590.68, respectively which are lower than previous experiment result. The grey line shows a 70% intensity of the maximum intensity. 10% of the maximum intensity is not achievable as corresponding integration time can't detect any droplet. All the other things are as similar to Figure 26.
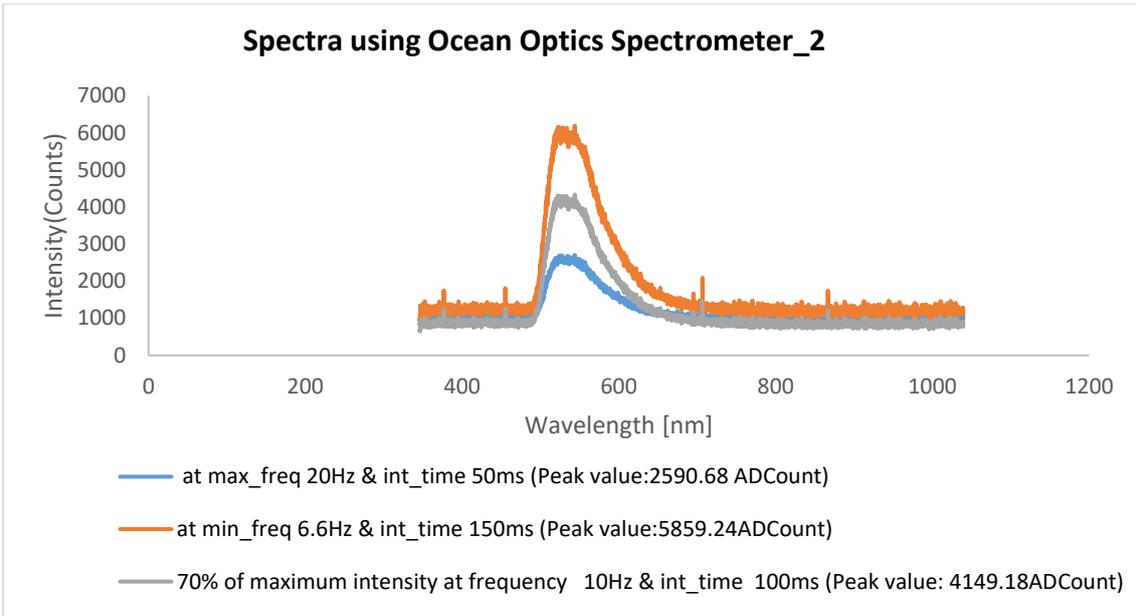
Figure 27. The spectrum captured using Ocean Optics spectrometer (II), the highest intensity is obtained at 6.6 Hz, and the lowest intensity is obtained at 20Hz frequency. The grey plot shows 70% of the maximum intensity.

The measurement data has been shown in Table 9 for synchronized maximum excitation signal frequency and integration time. From which single droplet detection speed and maximum amount of droplet detection in one second could find out.

Table 17. Summary of the measurements

Spectrometer	Maximum Frequency [Hz]	Integration Time [ms]	Droplet Detection per Second
Ocean optics spectrometer (I)	20	50	20
Ocean optics spectrometer (II)	20	50	20
Avantes Specrometer (III)	500	2	500

Hamamatsu spectrometer (IV)	5000	0.2	5000

For instance, row 1 and 2 interpret that excitation frequency is 20 Hz, and integration time is 50ms, which means detector can detect a single droplet in 50ms. In other words, the detector can detect a maximum of 20 droplets in one second. For the third spectrometer, single droplet detection takes 2ms time; thus, in one second, it can detect 500 droplets. And finally, the fourth spectrometer (Hamamatsu Spectrometer) can detect a maximum of 5000 droplets in one second because single droplet detection takes 0.2ms time.

Summarily, it can be concluded that the Hamamatsu spectrometer is better for our use case than three other spectrometers as it can detect a single droplet faster. But this amount is meagre in comparison with recent flow cytometer development. Hence further investigation is required, which would be the future work.

5 Summary and Conclusion

The aim of the thesis work is fulfilled by analysing the sensitivity and detection speed of the spectrometers. A state-of-the-art overview was given on the excitation and detection part of a flow cytometer for lab-on-a-chip technology, showing the possible solution for optical path development. The requirements for the analysis setup have been assessed from Thomas Johann Seebeck Department of Electronics Lab-on-a-Chip. In the materials and methods section of the thesis, the action plan was discussed, explaining all the major component choices and evaluating the key requirements for the electronics. A setup was constructed to find out the sensitivity of the spectrometer and the most powerful light source. To find out the spectrometer detection speed, another setup was designed with suitable cuvette holder, light source and spectrometer together, all integrated into a simple enclosure for measurement and analysis of the concept. Instead of the droplet, a sinusoidal signal was used to reduce the time in evaluation and further development of the device. An Agilent DSO-X 2012A Digital Storage Oscilloscope was used to measure the amplitude of the waveform. The spectra were measured through vendor-specific software for each spectrometer in a PC. The additional electronics design was constructed for the purpose of constant intensity of the light. The software and communication option for different spectrometers also investigated for further automation possibility. Tests were carried out throughout the operating ambient temperature.

In conclusion, the results of the experimental analysis showed that the prototype based on modular commercial spectrometer is not capable of high throughput droplet detection, which leads to further investigation for development.

5.1 Further Development

As the prototype developed in this thesis needs further future development, most of the possible additions are related to the sensor replacement process. Including a semiconductor laser diode (LD) would give strong luminescence as a light source. Finding out the proper sensor for detecting single droplet in considerable speed is

another task for further development. These processes could include FEM simulation for optimization of the optical path before building next prototypes.

Lastly, this thesis is a milestone in a longer development process. Much of the work that needs to be done includes the investigation of additional components, finding out the signal to noise ratio and spatial resolution of the detector, etc. Beyond the development of the designs and processes, cost and miniaturization should be taken into account.

References

[1] W. R. Loewenstein, Y. Kanno, J. Gen, and W. R. Loewenstein, "Department of Physiology, College of Physicians and Surgeons, Columbia University, New York," p. 2.

[2] X. Li *et al.*, "A Microfluidic Flow Cytometry Enabling Absolute Quantification of Single-Cell Intracellular Proteins," *Lab Chip*, vol. 16, no. 1, pp. 75–85, 2016.

[3] C.-S. Yan and Y.-N. Wang, "Multi-parameter analysis using photovoltaic cell-based optofluidic cytometer," *Biomed. Opt. Express*, vol. 7, no. 9, p. 3585, Sep. 2016.

[4] F. Caselli and P. Bisegna, "Simulation and performance analysis of a novel high-accuracy sheathless microfluidic impedance cytometer with coplanar electrode layout," *Medical Engineering & Physics*, vol. 48, pp. 81–89, Oct. 2017.

[5] J. Liu, Y. Qiang, O. Alvarez, and E. Du, "Electrical impedance microflow cytometry with oxygen control for detection of sickle cells," *Sensors and Actuators B: Chemical*, vol. 255, pp. 2392–2398, Feb. 2018.

[6] R. Friedrich *et al.*, "A nano flow cytometer for single lipid vesicle analysis," *Lab Chip*, vol. 16, no. 1, pp. 75–85, 2016.

[7] Z. T. F. Yu *et al.*, "Centrifugal microfluidics for sorting immune cells from whole blood," *Sensors and Actuators B: Chemical*, vol. 245, pp. 1050–1061, Jun. 2017.

[8] H. Mikami *et al.*, "Ultrafast confocal fluorescence microscopy beyond the fluorescence lifetime limit," *Optica*, vol. 5, no. 2, p. 117, Feb. 2018.

[9] Accessed: Apr. 22, 2020. [Online]. Available: https://benchling.com/pub/tabor-flowcal.

[10] P. Kumar, "Biophysics and Molecular Biology," p. 101.

[11] A. B. Shrirao *et al.*, "Microfluidic flow cytometry: The role of microfabrication methodologies, performance and functional specification," *Technology*, vol. 06, no. 01, pp. 1–23, Mar. 2018.

[12] Y. Liu and X. Jiang, "Why microfluidics? Merits and trends in chemical synthesis," *Lab Chip*, vol. 17, no. 23, pp. 3960–3978, 2017.

[13] G. M. Whitesides, "The origins and the future of microfluidics," *Nature*, vol. 442, no. 7101, pp. 368–373, Jul. 2006.

[14] Md. M. Islam, A. Loewen, and P. B. Allen, "Simple, low-cost fabrication of acrylic based droplet microfluidics and its use to generate DNA-coated particles," *Sci Rep*, vol. 8, no. 1, p. 8763, Dec. 2018.

[15] B. L. Fiedler *et al.*, "Droplet Microfluidic Flow Cytometer For Sorting On Transient Cellular Responses Of Genetically-Encoded Sensors," *Anal. Chem.*, vol. 89, no. 1, pp. 711–719, Jan. 2017.

[16] "Flow Cytometry: Cell Analysis vs. Cell Sorting | Products | Bio-Rad." Accessed: Apr. 22, 2020. Online. Available: https://www.bio-rad.com/featured/en/flow-cytometer.html.

[17] I. Eriksson, K. Öllinger, and H. Appelqvist, "Analysis of Lysosomal pH by Flow Cytometry Using FITC-Dextran Loaded Cells," in *Lysosomes*, vol. 1594, K. Öllinger and H. Appelqvist, Eds. New York, NY: Springer New York, pp. 179–189, 2017.

[18] On behalf of the EuroFlow Consortium (EU-FP6, LSHB-CT-2006-018708) *et al.*, "EuroFlow standardization of flow cytometer instrument settings and immunophenotyping protocols," *Leukemia*, vol. 26, no. 9, pp. 1986–2010, Sep. 2012.

[19] H. Degheidy, S. Bauer, G. Marti, and L. Wang, "Flow Cytometer Performance Characterization, Standardization and Calibration against CD4 on T Lymphocytes Enables Quantification of Biomarker Expressions for Immunological Applications," *JBiSE*, vol. 07, no. 09, pp. 756–768, 2014.

[20] P. R. Errante, P. C. C. Ebbing, F. S. M. Rodrigues, R. R. N. Ferraz, and N. P. Da Silva, "Flow cytometry: a literature review," *cmbio*, vol. 14, no. 2, p. 221, Feb. 2016.

[21] T. S. Kaminski, O. Scheler, and P. Garstecki, "Droplet microfluidics for microbiology: techniques, applications and challenges," *Lab on a Chip*, vol. 16, no. 12, pp. 2168–2187, 2016.

[22] J. Picot, C. L. Guerin, C. Le Van Kim, and C. M. Boulanger, "Flow cytometry: retrospective, fundamentals and recent instrumentation," *Cytotechnology*, vol. 64, no. 2, pp. 109–130, Mar. 2012.

[23] E. Du, S. Ha, M. Diez-Silva, M. Dao, S. Suresh, and A. P. Chandrakasan, "Electric impedance microflow cytometry for characterization of cell disease states," *Lab on a Chip*, vol. 13, no. 19, p. 3903, 2013.

[24] S. Stavrakis, G. Holzner, J. Choo, and A. deMello, "High-throughput microfluidic imaging flow cytometry," *Current Opinion in Biotechnology*, vol. 55, pp. 36–43, Feb. 2019.

[25] R.-J. Yang, L.-M. Fu, and H.-H. Hou, "Review and perspectives on microfluidic flow cytometers," *Sensors and Actuators B: Chemical*, vol. 266, pp. 26–45, Aug. 2018.

[26] A. Adan, G. Alizada, Y. Kiraz, Y. Baran, and A. Nalbant, "Flow cytometry: basic principles and applications," *Critical Reviews in Biotechnology*, vol. 37, no. 2, pp. 163–176, Feb. 2017.

[27] A. Negron *et al.*, "Using flow cytometry and light-induced fluorescence to characterize the variability and characteristics of bioaerosols in springtime in Metro Atlanta, Georgia," *Atmos. Chem. Phys.*, vol. 20, no. 3, pp. 1817–1838, Feb. 2020.

[28] M. E. Piyasena and S. W. Graves, "The intersection of flow cytometry with microfluidics and microfabrication," *Lab Chip*, vol. 14, no. 6, pp. 1044–1059, 2014.

[29] M. A. Naivar *et al.*, "Development of small and inexpensive digital data acquisition systems using a microcontroller-based approach," *Cytometry Part A*, vol. 75A, no. 12, pp. 979–989, Dec. 2009.

[30] D. E. Moore, "System and method for managing data from a flow analyzer," no. US7274316B2, p. 9, 2015.

[31] H. Mikami *et al.*, "Virtual-freezing fluorescence imaging flow cytometry," *Nat Commun*, vol. 11, no. 1, p. 1162, Dec. 2020.

[32] M. Lippeveld *et al.*, "Classification of Human White Blood Cells Using Machine Learning for Stain-Free Imaging Flow Cytometry," *Cytometry*, vol. 97, no. 3, pp. 308–319, Mar. 2020.

[33] Y. Gong, N. Fan, X. Yang, B. Peng, and H. Jiang, "New advances in microfluidic flow cytometry," *ELECTROPHORESIS*, vol. 40, no. 8, pp. 1212–1229, Apr. 2019.

[34] X.-X. Fang, H.-Y. Li, P. Fang, J.-Z. Pan, and Q. Fang, "A handheld laser-induced fluorescence detector for multiple applications," *Talanta*, vol. 150, pp. 135–141, Apr. 2016.

[35] X. Geng, M. Shi, H. Ning, C. Feng, and Y. Guan, "A compact and low-cost laser induced fluorescence detector with silicon based photodetector assembly for capillary flow systems," *Talanta*, vol. 182, pp. 279–284, May 2018.

[36] S. K. Narayana, S. Mallick, H. Siegumfeldt, and F. van den Berg, "Bacterial Flow Cytometry and Imaging as Potential Process Monitoring Tools for Industrial Biotechnology," *Fermentation*, vol. 6, no. 1, p. 10, Jan. 2020.

[37] D.-K. Kang *et al.*, "3D Droplet Microfluidic Systems for High-Throughput Biological Experimentation," *Analytical Chemistry*, vol. 87, no. 21, pp. 10770–10778, Nov. 2015.

[38] Y. Wang *et al.*, "Time-resolved microfluidic flow cytometer for decoding luminescence lifetimes in the microsecond region," *Lab Chip*, vol. 20, no. 3, pp. 655–664, 2020.

[39] E. Schonbrun, S. S. Gorthi, and D. Schaak, "Microfabricated multiple field of view imaging flow cytometry," *Lab Chip*, vol. 12, no. 2, pp. 268–273, 2012.

[40] A. Hossain, J. Canning, S. Ast, P. J. Rutledge, Teh Li Yen, and A. Jamalipour, "Lab-in-a-Phone: Smartphone-Based Portable Fluorometer for pH Measurements of Environmental Water," *IEEE Sensors Journal*, vol. 15, no. 9, pp. 5095–5102, Sep. 2015.

[41] V. Yelleswarapu, J. R. Buser, M. Haber, J. Baron, E. Inapuri, and D. Issadore, "Mobile platform for rapid sub–picogram-per-milliliter, multiplexed, digital droplet detection of proteins," *Proc Natl Acad Sci USA*, vol. 116, no. 10, pp. 4489–4495, Mar. 2019.

[42] E. Kantzas, A. J. S. McGonigle, and R. Bryant, "Comparison of Low Cost Miniature Spectrometers for Volcanic SO2 Emission Measurements," *Sensors*, vol. 9, no. 5, pp. 3256–3268, Apr. 2009.

[43] J. Juola, "Prototyping electronics and software for a spectrometer module," p. 62.

[44] "Ocean-Optics-Inc-Ocean-Optics-USB4000-Fiber-Optic-Spectrometer-Fiber-Optic Center.pdf." Accessed: Apr. 27, 2020. [Online]. Available: http://focenter.com/wp-content/uploads/documents/Ocean-Optics-Inc-Ocean-Optics-USB4000-Fiber-Optic-Spectrometer-Fiber-Optic-Center.pdf.

[45] "avaspec-2048.pdf." Accessed: Apr. 27, 2020. [Online]. Available: http://telab.vuse.vanderbilt.edu/docs/specs/avaspec-2048.pdf.

[46] "c12880ma_kacc1226e.pdf." Accessed: Apr. 27, 2020. [Online]. Available: https://www.hamamatsu.com/resources/pdf/ssd/c12880ma_kacc1226e.pdf.

[47] "AvaLight-HAL-CAL-Mini and DH-CAL Calibrated Light Sources-Avantes." Accessed: Apr. 27, 2020. [Online]. Available: https://www.avantes.com/products/light-sources/item/947-avalight-hal-cal-mini-dh-cal-calibrated-light-source.

[48] "95-96_-_AvaLight-HAL-DH-CAL.pdf." Accessed: Apr. 27, 2020. [Online]. Available: http://www.avantes.com/images/stories/brochurescat2012/95-96_-_AvaLight-HAL-DH-CAL.pdf.